Manuscript ID: hess-2019-434

RESPONSES TO REVIEWER #1's COMMENTS

We are grateful to Reviewer #1 for his/her insightful review. The provided comments have contributed substantially to improving the paper. According to them, we have made significant efforts to revise the manuscript, with the details explained as follows:

Point #1
COMMENT:
only one error in the equation I could find (line 331, the dot normally indicating placement of index "l" should not be there)

RESPONSE: We are thankful for the reviewer's carefulness, and have corrected this part as follows:
Figure 1 show the locations of these three gauging stations based on the daily stream flow data

Point #2
COMMENT:
a question on whether all those significant digits are actually warranted in Tables 2-6 and in Figures 10-13.
.
RESPONSE: We appreciate the reviewer's comment. The digits in Tables 2-3 and Figures 10-13 are rounded in Excel, and the digits in Tables 4-6 are generated by the Design-Experts. All those significant digits can be warranted.

Point #3
COMMENT:
Figure 1 could be expanded I would argue to explicitly indicate copulas, etc and provide a few more details on the framework.

RESPONSE: We are grateful for the reviewer's suggestion. Firstly, we rename the full-subsampling factorial copula method to iterative factorial copula, which is more concise. Also, the full-subsampling factorial analysis is renamed as iterative factorial analysis. Also, we have provided more details for Figure 1 as follows:

Figure 1 illustrates the framework of the proposed IFC approach. The framework consists of four modules: (i) selection of marginal distributions, (ii) identification of copulas, (iii) parameter uncertainty quantification, (iv) parameter interaction and sensitivity analysis. In IFC, modules (i) and (ii) are proposed to construct the most appropriate copula-based hydrologic risk model. In detail, a number of distributions, such as Gamma, generalized extreme value (GEV), lognormal (LN), Pearson type III (P III), and log-Pearson type III (LP III) distributions, are usually employed to describe the probabilistic features of individual random variables (e.g. flood peak and volume). Also, in order to quantify the dependence structures of correlated random variables, many copula functions have been proposed, such as Gaussian copula, Student t copula, Archimedean copula family (e.g. Clayton, Gumbel, Frank and Joe copulas). In

the current study, the indices of root mean square errors (RMSE) and Akaike information criterion (AIC) will be employed to identify the most appropriate model for hydrologic risk inference. Module (iii) quantifies parameter uncertainties in marginal distributions and copulas. Modules (iv) would be the core part of our study to identify the main sources of uncertainties in multivariate risk inference by the proposed iterative factorial analysis (IFA) approach.

Point #4
COMMENT:
The two watersheds selected are not very different but you find discrepancies between which copulas perform best on which stations (lines 409 to 412) for predicting flood peak and volume, and different copulas are chosen to characterize uncertainty in the risks for each station (line 414-416). The authors are using data driven methods that have no explicit consideration for causal mechanisms (as with most data driven methods) but surely the differences in copulas selected are caused by physical differences in the watersheds. Can the authors please explain these discrepancies in terms of physical watershed characteristics (or perhaps make the case for why the differences cannot be ascribed to physical differences)?

RESPONSE: We are thankful for the reviewer's suggestion. We have added discussion for this issue in Section 5.1 as follows:

5.1. Differences for the Hydrologic Risk Models at Different Stations

Different copula functions are applied for different stations, which are chosen based on the indices of RMSE and AIC. However, the selection of copula models at different stations may also be related with some key characteristics of the drainage areas for those stations. The Gumbel copula will be applied for the Zhangjiashan station. It can reflect strong correlation at high values. However, the Joe copula, which is adopted for the Xianyang station, can reflect stronger right tail positive dependence. Both the Xianyang and Zhangjiashan stations have similar drainage areas. The Xianyang station controls a drainage area of 46,480 km^2 (Xu et al., 2016), while the Zhangjiashan station has a drainage area of 45,412 km^2 (Sun et al., 2019). Nevertheless, the major reason that lead to different copula functions for these two stations may be due to the elevation features for those two drainage areas. The drainage area of Zhangjiashan station is located in the central part of Loess Plateau of China and thus the major part of this drainage area is a mountainous region. In comparison, even thought a large part of the drainage area of Xianyang station is also located in the mountainous region, the Xianyang station also controls a significant part of the Guanzhong Plain, as indicated in the red part of Figure 2. Consequently, the flood hydrograph at Zhangjiashan station may be sharp while the flood hydrograph at Xianyang station is relatively flat and show a stronger right tail dependence among flood peak and volume. In fact, the value of Kendall's tau between peak and volume for the top ten floods at Zhangjiashan station is 0.33 while such a value of Kendall's tau at Xianyang station is 0.6. These facts may explain the Gumbel copula is applicable for Zhangjiashan station while the Joe copula is applied for Xianyang station.

Point #4

COMMENT:
Please detail what part of the analyses is watershed specific and thus, what analysis should each user conduct each time and for every station they wish to understand prediction uncertainty and parameter interaction with the outcomes of their analyses; or conversely, what can they simply adopt from the Tables and Figures for their watersheds

RESPONSE: We are grateful for the reviewer's suggestion. This study aims to propose a reliable uncertainty partition method for multivariate risk inference. Based on this method, the decision maker can track the major sources for the uncertainties in the risk inferences. The proposed method can be applied for different watersheds. We have highlight the usefulness of our study in conclusions as follows:

> The proposed method has been applied for flood risk inferences at two gauge stations in Wei River basin. The results indicate that uncertainties in the parameters of the copula-based model would lead to noticeable uncertainties in the resulting risk inferences, especially for the joint flood risk in AND. noticeable uncertainties exist in the predictive joint RP of AND even for a small flood event. However, the results from IFA suggested that those uncertainties in risk inferences may mainly be attributed to the uncertainties in shape parameter in GEV distribution and the parameter of sdlog in LN for both the two stations. In comparison, the parameter uncertainty in the copula function would not pose an obvious effect on the resulting uncertainty in risk inferences. Such results indicate that, at least that the Wei River basin, the decision makers need to well estimate the values or quantify the uncertainties for the shape parameter in GEV distribution and sdlog in the LN distribution, in order to obtain reliable risk inferences. For other catchments, the proposed IFC method can be adopted to reveal the major sources for uncertainties in risk inferences and then provide potential pathways to get reliable risk inferences.

RESPONSES TO REVIEWER #2's COMMENTS

We are grateful to Reviewer #2 for his/her insightful review. The provided comments have contributed substantially to improving the paper. According to them, we have made significant efforts to revise the manuscript, with the details explained as follows:

Point #1
COMMENT:
detailed comments in the marked up version

RESPONSE: We are really thankful for the reviewer's carefulness and comments. We have revised all the errors in our manuscript carefully which have been highlighted in the revision

Point #2
COMMENT:
There is something missing here. Please introduce your 'OR' and 'AND' cases to assist the reader. Also, what are the names of T^{OR} and T^{AND}? what do they describe? What is R^d?

RESPONSE: We appreciate the reviewer's comment. We have provided more details about the joint return period in OR and AND as follows:

(i) "OR" case T^{OR}:

$$T^{OR} = \{(x_1, x_2, ..., x_d) \in R^d : x_1 > x_1^* \lor x_2 > x_2^* \lor ... \lor x_d > x_d^*\}$$
$$= \frac{\mu}{1 - C(F_1(x_1 \mid \gamma_1), ..., F_d(x_d \mid \gamma_d) \mid \theta)} \tag{4}$$

where R^d is a d-dimensional real space; μ denotes the average time between two adjacent events under consideration. The joint RP in OR (denoted as T^{OR}) indicates the occurrence probability of the extreme event with one of its variables x_i's, $i = 1, 2, …, d$, exceeding the corresponding threshold x_i^*

(ii) "AND" case T^{AND}:

$$T^{AND} = \{(x_1, x_2, ..., x_d) \in R^d : x_1 > x_1^* \land x_2 > x_2^* \land ... \land x_d > x_d^*\}$$
$$= \frac{\mu}{\hat{C}(\overline{F}_1(x_1 \mid \gamma_1), \overline{F}_2(x_2 \mid \gamma_2), ..., \overline{F}_1(x_d \mid \gamma_d) \mid \theta)} \tag{5}$$

where $\hat{C}$ is the multivariate survival function of the X_i's proposed by Salvadori et al. (2013;

2016), and $\overline{F}_i(x_i \mid \gamma_i) = P(X > x_i) = 1 - F_i(x_i \mid \gamma_i)$. Following Salvadori et al. (2013; 2016), and

the Inclusion-Exclusion principle proposed by Joe (2014), the multivariate survival function $\hat{C}$ can be obtained by:

$$\hat{C}(\mathbf{u}) = \overline{C}(1-\mathbf{u}) \tag{6}$$

and

$$\overline{C}(\mathbf{u}) = 1 - \sum_{i=1}^{d} u_i + \sum_{S \in P}(-1)^{\#(S)} C_S(u_i : i \in S) \tag{7}$$

where $\#(S)$ denotes the cardinality of S. The joint RP in AND (denoted as T^{AND}) of the extreme event indicates the occurrence probability with all of its variables x_i's, $i = 1, 2, \ldots, d$, exceeding the corresponding thresholds x_i^*'s

Point #3
COMMENT:
In order to be accurate, Figs 10 to 12 are tables and should be labelled and referred to as such

RESPONSE: We are grateful for the reviewer's comment. Figures 10 – 12 show the contributions of model parameters to uncertainties in risk inferences under different design standards and service time periods. These results seem to be presented in tables. However, Figures 10-12 are in fact heat maps generated by Excel, in which different parameter contributions are highlighted by different colors. Consequently, we labelled them as figures rather than tables.

An Uncertainty Partition Approach for Inferring Interactive Hydrologic Risks

Yurui Fan[1], Kai Huang[2], Guohe Huang[3], Yongping Li[4], Feng Wang[4]

[1] Department of Civil and Environmental Engineering, Brunel University, London, Uxbridge, Middlesex, UB8
  3PH, United Kingdom
[2] Faculty of Engineering and Applied Sciences, University of Regina, Regina, SK, Canada, S4S0A2
[3] Institute for Energy, Environment and Sustainable Communities, University of Regina, Regina, Saskatchewan,
  Canada S4S 0A2
[4] School of Environment, Beijing Normal University, Beijing 100875, China

Correspondence to: Yurui Fan (yurui.fan@brunel.ac.uk), Guohe Huang (huangg@uregina.ca)

Abstract:

Extensive uncertainties exist in hydrologic risk analysis. Particularly for interdependent hydrometeorological extremes, the random features in individual variables and their dependence structures may lead to bias and uncertainty in future risk inferences. In this study, an iterative factorial copula (IFC) approach is proposed to quantify parameter uncertainties and further reveal their contributions to predictive uncertainties in risk inferences. Specifically, an iterative factorial analysis (IFA) approach is developed to diminish the effect of the sample size and provide reliable characterization for parameters' contributions to the resulting risk inferences. The proposed approach is applied to multivariate flood risk inference for the Wei River basin to demonstrate the applicability of IFC for tracking the major contributors to resulting uncertainty in a multivariate risk analysis framework. In

detail, the multivariate risk model associated with flood peak and volume will be established and further introduced into the proposed iterative factorial analysis framework to reveal the individual and interactive effects of parameter uncertainties on the predictive uncertainties in the resulting risk inferences. The results suggest that uncertainties in risk inferences would mainly be attributed to some parameters of the marginal distributions while the parameter of the dependence structure (i.e. copula function) would not produce noticeable effects. Moreover, compared with traditional factorial analysis (FA), the proposed IFA approach would produce a more reliable visualization for parameters' impacts on risk inferences, while the traditional FA would remarkably overestimate the contribution of parameters' interaction to the failure probability in AND (i.e. all variables would exceed the corresponding thresholds), and at the same time, underestimate the contribution of parameters' interaction to the failure probabilities in OR (i.e. one variable would exceed its corresponding threshold) and Kendall (i.e. the correlated variables would exceed a critical multivariate threshold).

1. Introduction

Many hydrological and climatological extremes are highly correlated among each other, and it is desired to explore their interdependence through multivariate approaches. Examples include sea level rise and fluvial flood (Moftakhari et al., 2017), drought and heat waves (Sun et al., 2019), soil moisture and precipitation (AghaKouchak, 2015). Moreover, even one specific hydrological extreme may have multiple attributes, such as the peak and volume for a flood, duration and severity for a drought, and duration and intensity of a storm (Karmakar

and Simonovic, 2009; Kong et al., 2019). Traditional univariate approaches, mainly focusing on one variable or one attribute of hydrological extremes (e.g. flood peak), may not be sufficient to describe those hydrological extemes containing multivariate characteristics. Thus the univariate frequency/risk analysis methods may be unable to obtain reliable risk

55   inferences for the failure probability or recurrence intervals of interdependent extreme events (Chebana and Ouarda, 2011; Requena et al., 2013; Salvadori et al., 2016; Sadegh et al., 2017)

Since the introduction of the copula function into hydrology and geosciences by De Michele and Salvadori (2003), the copula-based approaches have been widely used for multivariate

60   hydrologic risk analysis. The copula functions are able to model correlated variables with complex or nonlinear dependence structures. Also, these kinds of methods are easily implemented since the marginal distributions and dependence models can be estimated in separate processes, which also give flexibility in the selection of both marginal and dependence models. A large amount of research has been developed for multivariate

65   hydrologic simulation through copula functions, such as multivariate flood frequency analysis (Sraj et al., 2014; Xu et al., 2016; Fan et al., 2018, 2020); drought assessments (Song and Singh 2010; Kao and Govindaraju 2010; Ma et al. 2013); storm or rainfall dependence analysis (Zhang and Singh 2007; Vandenberghe et al. 2010); streamflow simulation (Lee and Salas 2011; Kong et al., 2015) and other water and environmental engineering applications

70   (Fan et al., 2017; Huang et al., 2017).

For both univariate and multivariate analyses for hydrometeorological risks, uncertainty would be one of the unavoidable issues which needs to be well addressed. The uncertainty in

3

hydrometeorological risk inference mainly results from stochastic variability of

75　hydrometeorological processes and incomplete knowledge of the watershed systems (Merz and Thieken, 2005). Many studies have been proposed to address uncertainty in both univariate and multivariate hydrological risk analysis (e.g. Merz and Thieken, 2005; Serinaldi, 2013; Dung et al., 2015; Zhang et al., 2015; Sadegh et al., 2017; Fan et al., 2018). However, one critical issue in uncertainty quantification of hydrological inference is how to

80　characterize the major sources for uncertain risk inference. Qi et al. (2016) employed a subsampling ANOVA approach (Bosshard et al., 2013) to quantify individual and interactive impacts of the uncertainties in data, probability distribution functions and probability distribution parameters, on the total cost for flood control in terms of flood peak flows. Even though the subsampling ANOVA approach is able to reduce the effect of the biased estimator

85　on quantification of variance contribution resulting from the traditional ANOVA approach, it should be noticed that merely subsampling one uncertainty parameter/factor (referred as single-subsampling ANOVA), as used in the studies by Bosshard et al. (2013) and Qi et al. (2016a), will lead to (i) an underestimation of the individual contribution for the factor to be sampled and (2) overestimation of contributions from those non-sampled factors. Moreover,

90　few studies have been reported to characterize the individual and interactive effects of parameter uncertainties in marginal and dependence models on the multivariate risk inferences.

Consequently, as an extension of previous research, this study aims to propose an iterative

95　factorial copula (IFC) approach for quantifying and partitioning uncertainty metrics from different sources in multivariate hydrologic risk inference. In detail, the parameter

4

uncertainties are quantified through a Monte Carlo-based Bootstrap algorithm. The interactions of parameter uncertainties are explored through a multilevel factorial analysis approach. The contributions of parameter uncertainties are analyzed through an iterative

100   factorial analysis (IFA) method, in which all uncertainty factors will be subsampled to generate more reliable results. The applicability of the proposed IFC approach will be demonstrated through case studies of flood risk analysis in the Wei River basin in China.

2. Methodology

105   Figure 1 illustrates the framework of the proposed IFC approach. The framework consists of four modules: (i) selection of marginal distributions, (ii) identification of copulas, (iii) parameter uncertainty quantification, and (iv) parameter interaction and sensitivity analysis. In IFC, modules (i) and (ii) are proposed to construct the most appropriate copula-based hydrologic risk model. In detail, a number of distributions, such as Gamma, generalized

110   extreme value (GEV), lognormal (LN), Pearson type III (P III), and log-Pearson type III (LP III) distributions, are usually employed to describe the probabilistic features of individual random variables (e.g. flood peak and volume). Also, in order to quantify the dependence structures of correlated random variables, many copula functions have been proposed, such as Gaussian copula, Student t copula, Archimedean copula family (e.g. Clayton, Gumbel, Frank

115   and Joe copulas). In the current study, the indices of root mean square errors (RMSE) and Akaike information criterion (AIC) will be employed to identify the most appropriate model for hydrologic risk inference. Module (iii) quantifies parameter uncertainties in marginal distributions and copulas. Modules (iv) would be the core part of our study to identify the

120

\-

Place Figure 1 here

\-

125

2.2. Copula-based Multivariate Risk Inference Framework

A copula function is a multivariate distribution function with uniform margins on the interval
[0, 1]. Sklar's Theorem states that any d-dimensional distribution function F can be

130   formulated through a copula and its marginal distributions (Nelsen, 2006). In detail, a
multivariate copula function can be expressed as:

$$F(x_1, x_2, ..., x_d \mid \gamma_1, \gamma_2, ..., \gamma_d, \theta) = C(F_{X_1}(x_1 \mid \gamma_1), F_{X_2}(x_2 \mid \gamma_2), ..., F_{X_d}(x_d \mid \gamma_d) \mid \theta) \qquad (1)$$

where $F_{X_1}(x_1 \mid \gamma_1), F_{X_2}(x_2 \mid \gamma_2), ..., F_{X_d}(x_d \mid \gamma_d)$ are marginal distributions of the random vector

$(X_1, X_2, ..., X_d)$, with $\gamma_1, \gamma_2, ..., \gamma_d$ respectively being the unknown parameters of the marginal

135   distributions. θ is the parameter in the copula function describing dependence among the
correlated variables. If these marginal distributions are continuous, then a single copula
function C exists, which can be written as (Nelsen, 2006):

$$C(u_1, u_2, ..., u_d \mid \theta) = F(F_{X_1}^{-1}(u_1 \mid \gamma_1), F_{X_2}^{-1}(u_2 \mid \gamma_2), ..., F_{X_d}^{-1}(u_d \mid \gamma_d)) \qquad (2)$$

where $u_1 = F_{X_1}(x_1 \mid \gamma_1)$, $u_2 = F_{X_2}(x_2 \mid \gamma_2)$, ..., $u_d = F_{X_d}(x_d \mid \gamma_d)$. More details on the

140   theoretical background and properties of various copula families can be found in Nelsen (2006).

If appropriate copula functions are specified to reflect the joint probabilistic characteristics for a multivariate extreme event, the conditional, primary and secondary return periods (RP) can be obtained. Consider one kind of hydrological extreme (denoted as X) with d attributes

145   (i.e. $X = (x_1, x_2, \ldots, x_d)$), and for a specific extreme event X^* with its attributes being $X^* = (x_1^*, x_2^*, \ldots, x_d^*)$), three categories of multivariate RP can be applied for determining the potential risk of X^*.

(i) "OR" case T^{OR}:

$$T^{OR} = \{(x_1, x_2, \ldots, x_d) \in R^d : x_1 > x_1^* \vee x_2 > x_2^* \vee \ldots \vee x_d > x_d^*\}$$

150
$$= \frac{\mu}{1 - C(F_1(x_1 \mid \gamma_1), \ldots, F_d(x_d \mid \gamma_d) \mid \theta)} \tag{4}$$

where R^d is a d-dimensional real space; μ denotes the average time between two adjacent events under consideration. The joint RP in OR (denoted as T^{OR}) indicates the occurrence probability of the extreme event with one of its variables x_i's, $i = 1, 2, \ldots, d$, exceeding the corresponding threshold x_i^*

155

(ii) "AND" case T^{AND}:

$$T^{AND} = \{(x_1, x_2, \ldots, x_d) \in R^d : x_1 > x_1^* \wedge x_2 > x_2^* \wedge \ldots \wedge x_d > x_d^*\}$$

$$= \frac{\mu}{\hat{C}(\overline{F}_1(x_1 \mid \gamma_1), \overline{F}_2(x_2 \mid \gamma_2), \ldots, \overline{F}_1(x_d \mid \gamma_d) \mid \theta)} \tag{5}$$

7

where $\hat{C}$ is the multivariate survival function of the X_i's proposed by Salvadori et al. (2013; 2016), and $\overline{F}_i(x_i \mid \gamma_i) = P(X > x_i) = 1 - F_i(x_i \mid \gamma_i)$. Following Salvadori et al. (2013; 2016),

160   and the Inclusion-Exclusion principle proposed by Joe (2014), the multivariate survival

function $\hat{C}$ can be obtained by:

$$\hat{C}(\mathbf{u}) = \overline{C}(1-\mathbf{u}) \tag{6}$$

and

$$\overline{C}(\mathbf{u}) = 1 - \sum_{i=1}^{d} u_i + \sum_{S \in P} (-1)^{\#(S)} C_S(u_i : i \in S) \tag{7}$$

165   where #(S) denotes the cardinality of S. The joint RP in AND (denoted as T^{AND}) of the extreme event indicates the occurrence probability with all of its variables x_i's, $i = 1, 2, \ldots, d$, exceeding the corresponding thresholds x_i^*'s

(iii) "Kendall" case: The Kendall RP characterizes the hydrologic disasters exceeding a

170   critical layer as defined by (Salvadori et al., 2011): $L_t^F = \{\boldsymbol{x} \in R^d : F(\boldsymbol{x}) = t\}$. The Kendall RP

can be expressed as (Salvadori et al., 2011):

$$T^{Kendall} = \frac{\mu}{1 - K_C(t)} \tag{8}$$

where K_C is the Kendall distribution function associated with the copula C, which can be expressed as:

175    $$K_C(t) = P(C(F_1(x_1 \mid \gamma_1), \ldots, F_d(x_d \mid \gamma_d) \mid \theta) \le t) \tag{9}$$

In addition to the multivariate RP, Failure probability (FP) can be another index to provide more coherent, general and well devised tools for multivariate risk assessment and communication. In general, the failure probability p_M to indicate the occurrence of a critical event for at least one time in M years of design life can be defined as (Salvadori et al., 2016):

$$p_M = 1 - \prod_{j=1}^{M}(1-p_j) = 1 - (F(x_d))^M \tag{10}$$

Similar to the multivariate RP concept, the failure probability in a multivariate context can also be characterized in "OR", "AND", and "Kendall" scenarios expressed by the following equations. For a given critical threshold $x^* = \{x_1^*, x_2^*, ..., x_d^*\}$, the failure probabilities violating this critical value can be expressed as (Salvadori et al., 2016):

$$p_T^{OR} = 1 - (C(F_1(x_1^*|\gamma_1), F_1(x_2^*|\gamma_2), ..., F_d(x_d^*|\gamma_d)|\theta))^T \tag{11a}$$

$$p_T^{AND} = 1 - (1 - \hat{C}(\overline{F}_1(x_1^*|\gamma_1), \overline{F}_2(x_2^*|\gamma_2), ..., \overline{F}_1(x_d^*|\gamma_d)|\theta))^T \tag{11b}$$

$$p_T^{Kendall} = 1 - (P(C(F_1(x_1^*|\gamma_1), F_1(x_2^*|\gamma_2), ..., F_d(x_d^*|\gamma_d)|\theta) \le t))^T \tag{11c}$$

where p_T^{OR}, p_T^{AND}, and $p_T^{Kendall}$ respectively denote the failure probability in "AND", "OR" and "Kendall" cases. T indicates the service time of the facilities under consideration.

Focusing on a bivariate case, the joint RP and the associated failure probability in "OR", "AND", and "Kendall" scenarios can be formulated as (Salvadori et al., 2007, 2011; Graler et al., 2013; Sraj et al., 2014; Serinaldi, 2015):

9

$$T^{OR}_{u_1,u_2} = \frac{\mu}{1 - C_{U_1U_2}(u_1, u_2 \mid \theta)} \tag{12a}$$

$$T^{AND}_{u_1,u_2} = \frac{\mu}{1 - u_1 - u_2 + C_{U_1U_2}(u_1, u_2 \mid \theta)} \tag{12b}$$

$$T^{Kendall}_{u_1,u_2} = \frac{\mu}{1 - P(C_{U_1U_2}(u_1^*, u_2^*) \leq t)} \tag{12c}$$

$$p_T^{OR} = 1 - (C_{U_1U_2}(u_1^*, u_2^* \mid \theta))^T \tag{12d}$$

$$p_T^{AND} = 1 - (u_1^* + u_2^* - \hat{C}_{U_1U_2}(u_1^*, u_2^* \mid \theta))^T \tag{12e}$$

$$p_T^{Kendall} = 1 - (P(C_{U_1U_2}(u_1^*, u_2^* \mid \theta) \leq t))^T \tag{12f}$$

where $u_1 = F_1(x_1 \mid \gamma_1), u_2 = F_2(x_2 \mid \gamma_2), \; u_1^* = F_1(x_1^* \mid \gamma_1), u_2^* = F_2(x_2^* \mid \gamma_2), (x_1^*, x_2^*)$ defines the bivariate threshold.

2.3. Uncertainty in the ==Copula-based== Risk Model

Extensive uncertainties may be involved in the parametric estimation of a copula function due to: (i) the inherent uncertainty in the flooding process; (ii) uncertainty in the selection of appropriate marginal functions and copulas; and, (iii) statistical uncertainty or parameter uncertainty within the parameter estimation process (e.g. the availability of samples) (Zhang et al., 2015). Several methods have been proposed to quantify parameter uncertainties in copula-based models. For instance, Dung et al. (2015) proposed bootstrap-based methods for

quantifying the parameter uncertainties in bivariate copula models. Zhang et al. (2015) employed a Bayesian inference approach for evaluating uncertainties in copula-based

215   hydrologic drought models, in which the Component-wise Hit-And-Run Metropolis algorithm is adopted to estimate the posterior probabilities of model parameters.

In this study, a bootstrap-based algorithm, is applied to quantify parameter uncertainties in the copula-based multivariate risk model. The procedures describing the bootstrap-based

220   algorithm to derive probabilistic distributions of the parameters in both marginal and dependence models are presented as follows:

1. Predefine a large number of bootstrapping samplings N_B

2. Implement the resampling with replacement over observed pairs $Z = (X, Y)$ to obtain $Z^* = (X^*, Y^*)$; Z^* has the same size as Z.

225   3. Fit the chosen marginal distributions to X^* and Y^*, and estimate the associated parameters (γ_X, γ_Y).

4. Fit the chosen copula to Z^*, and estimate the parameter in the copula function θ.

5. Repeat step 2–5 N_B times, and obtain N_B sets of $(\gamma_X, \gamma_Y, \theta)$. Moreover, in order to reject those parameters that lead to bad fits for both marginal and copula models, the A-D test and

230   the Cramer-von-Mises test are introduced in the bootstrap procedure to ensure that the obtained parameters can pass statistical tests for both the marginal distribution and copula models. Then the kernel method will be adopted to quantify the probabilistic features for $\gamma_X, \gamma_Y, \theta$.

6. In order to derive bivariate uncertainty bands for a predefined quantile curve (QC) with

235   certain joint RP in 'AND', 'OR' or 'Kendall' (denoted as T^{AND}, T^{OR}, $T^{Kendall}$), sample N_{B_1} sets

of $(\gamma_X, \gamma_Y, \theta)$ from the obtained N_B samples

7. Sample a large number (N_s) of $x_i\ y_j$ from their marginal distributions.

8. For each set of $(\gamma_X, \gamma_Y, \theta)$ from N_{B_1}, evaluate the joint RPs of (x_i, y_j) ($i = 1, 2, \ldots, N_s$; $y =$

1, 2, …, N_s), and store the pairs of (x_i, y_j) approaching the predefined joint RPs.

240   9. Repeat step 8 for N_{B_1}, and for each predefined QC, and plot the bivariate uncertainty

bands for each quantile QC

2.4. Interactive and Sensitivity Analysis for Parameter Uncertainties

245   Due to the uncertainties existing in <mark>the unknown values of</mark> parameters for a copula model, the

associated risk or the return period for a flooding event may also be uncertain. Few studies

have been reported to analyze the effect of uncertainties in the copula model on evaluating

the risk for a flood event. To address the above issue, an iterative factorial analysis (IFA)

approach will be proposed to reveal the individual and interactive effects of parameter

250   uncertainties on the predictive uncertainties of different risk inferences.

Consider a copula-based bivariate risk assessment model which has two marginal

distributions (A and B) and one copula (C). The parameters in the two marginal distributions

are assumed to be respectively denoted as γ^A with a levels and γ^B with b levels, while the

255   parameter in the copula is denoted with θ^C with c levels. The three factor ANOVA model for

such a factorial design in terms of the predictive risk (denoted as R) in response to the parameters γ_A, γ_B, θ_C and n replicates, can be expressed as:

$$R_{ijkl} = R_0 + R_{\theta_i^C} + R_{\gamma_j^A} + R_{\gamma_k^B} + R_{\theta_i^C \gamma_j^A} + R_{\theta_i^C \gamma_k^B} + R_{\gamma_j^A \gamma_k^B} + R_{\theta_i^C \gamma_j^A \gamma_k^B} + \varepsilon_{ijkl} \begin{cases} i = 1, 2, ..., c \\ j = 1, 2, ..., a \\ k = 1, 2, ...b \\ l = 1, 2, ..., n \end{cases} \quad (13)$$

260   where R_0 denotes the overall mean effect; $R_{\theta_i^C}, R_{\gamma_j^A}, R_{\gamma_k^B}$ respectively indicate the effect for

parameter θ^C in the copula at the ith level, parameter γ^A in the first marginal distribution at the jth level, and parameter γ^B in the first marginal distribution at the kth level; $R_{\theta_i^C \gamma_j^A}, R_{\theta_i^C \gamma_k^B}, R_{\gamma_j^A \gamma_k^B}$ indicate interactions between factors θ^C and γ^A, θ^C and γ^B, as well as γ^A and γ^B, respectively; $R_{\theta_i^C \gamma_j^A \gamma_k^B}$ denotes the interaction of factors θ^C, γ^A and γ^B; ε_{ijkl} denotes the random error

265   component.

Based on Equation (13), the total variability of the predictive risk can be decomposed into its component parts as follows (Montgomery, 2001):

270    $$SS_T = SS_{\theta^C} + SS_{\gamma^A} + SS_{\gamma^B} + SS_I + SS_e \quad (14a)$$

and

$$SS_T = \sum_{i=1}^{c} \sum_{j=1}^{a} \sum_{k=1}^{b} \sum_{l=1}^{n} R_{ijkl}^2 - \frac{R_{....}^2}{abcn} \quad (14b)$$

13

$$SS_{\theta^C} = \frac{1}{abn} \sum_{i=1}^{c} R_{i...}^2 - \frac{R_{....}^2}{abcn} \tag{14c}$$

$$SS_{\gamma^A} = \frac{1}{bcn} \sum_{j=1}^{a} R_{.j..}^2 - \frac{R_{....}^2}{abcn} \tag{14d}$$

$$SS_{\gamma^B} = \frac{1}{acn} \sum_{k=1}^{b} R_{..k.}^2 - \frac{R_{....}^2}{abcn} \tag{14e}$$

$$SS_e = \sum_{i=1}^{c}\sum_{j=1}^{a}\sum_{k=1}^{b}\sum_{l=1}^{n} R_{ijkl}^2 - \frac{1}{n}\sum_{i=1}^{c}\sum_{j=1}^{a}\sum_{k=1}^{b} R_{ijk.}^2 \tag{14f}$$

$$\begin{aligned} SS_I &= SS_{\theta^C \gamma^A} + SS_{\theta^C \gamma^B} + SS_{\gamma^B \gamma^A} + SS_{\theta^C \gamma^A \gamma^B} \\ &= SS_T - SS_{\theta^C} - SS_{\gamma^A} - SS_{\gamma^B} - SS_e \end{aligned} \tag{14g}$$

where $R_{ijk.} = \sum_{l=1}^{n} R_{ijkl}$, $R_{i...} = \sum_{j=1}^{a}\sum_{k=1}^{b}\sum_{l=1}^{n} R_{ijkl}$, $R_{.j..} = \sum_{i=1}^{c}\sum_{k=1}^{b}\sum_{l=1}^{n} R_{ijkl}$,

$R_{..k.} = \sum_{i=1}^{c}\sum_{j=1}^{a}\sum_{l=1}^{n} R_{ijkl}$ $R_{....} = \sum_{i=1}^{c}\sum_{j=1}^{a}\sum_{k=1}^{b}\sum_{l=1}^{n} R_{ijkl}$. Then the contributions of parameter

uncertainties in marginal distributions and dependence structures can be calculated as:

(1) Contribution of parameters in marginal distributions A and B

$$\eta_A = SS_{\gamma^A} / SS_T \tag{15a}$$

$$\eta_B = SS_{\gamma^B} / SS_T \tag{15b}$$

(2) Contribution of the parameter in the dependence structure

$$\eta_C = SS_{\theta^C} / SS_T \tag{15c}$$

(3) Contribution of internal variability

$$\eta_e = SS_e / SS_T \tag{15d}$$

(4) Contribution of parameter interactions

290 $$\eta_I = 1 - \eta_A - \eta_B - \eta_C - \eta_e \qquad\qquad\qquad (15e)$$

However, one major issue for the ANOVA approach is that the biased variance estimator in ANOVA would underestimate the variance in small sample size scenarios (Bosshard et al., 2013). Thus the sample size may significantly affect the resulting variance contributions

295 expressed in Equations (15a) – (15e). A subsampling approach has been advanced by Bosshard et al. (2013) to diminish the effect of the sample size in ANOVA and has been employed for uncertainty partitioning in flood design and hydrological simulation (Qi et al., 2016a, b). In such a subsampling scheme, one factor (denoted as X) with T levels (these levels can be different values for numerical parameters, or different types for non-numerical

300 factor (e.g. model type)), would choose two levels in each iteration. For T possible levels of X, we can obtain a total of C_T^2 possible pairs for X, expressed as a $2 \times C_T^2$ matrix as follows:

$$g(h, j) = \begin{pmatrix} X_1 & X_1 & \cdots & X_1 & X_2 & X_2 & \cdots & X_{T-2} & X_{T-2} & X_{T-1} \\ X_2 & X_3 & \cdots & X_T & X_3 & X_4 & \cdots & X_{T-1} & X_T & X_T \end{pmatrix} \qquad (16)$$

305

However, such a subsampling approach is mainly applied to subsample merely one factor or one parameter (here we refer to this method as single-subsampling ANOVA) in previous studies (Bosshard et al. 2013; Qi et al., 2016a, b). However, a critical issue for the single-subsampling ANOVA it that it will lead to an underestimation of the individual contribution

for the factor to be sampled and overestimation of contributions for those non-sampled factors. Consequently, in this study, we will propose an IFA approach to subsample all the factors to be addressed, and then quantify the contribution of each factor to the response variation. In the IFA approach, all factors under consideration will be subsampled, and the corresponding sum of squares will be obtained. The contribution of one factor would be characterized by the mean value of its contribution in each iteration. In detail, for the three factor ANOVA model expressed by Equation (13), the subsampling schemes for the three parameters can be formulated as:

$$
g_{\theta^C}(h_C, j_C) = \begin{pmatrix} \theta_1^C & \theta_1^C & \cdots & \theta_1^C & \theta_2^C & \theta_2^C & \cdots & \theta_{c-2}^C & \theta_{c-2}^C & \theta_{c-1}^C \\ \theta_2^C & \theta_3^C & \cdots & \theta_c^C & \theta_3^C & \theta_4^C & \cdots & \theta_{c-1}^C & \theta_c^C & \theta_c^C \end{pmatrix} \tag{17a}
$$

$$
g_{\gamma^A}(h_A, j_A) = \begin{pmatrix} \gamma_1^A & \gamma_1^A & \cdots & \gamma_1^A & \gamma_2^A & \gamma_2^A & \cdots & \gamma_{a-2}^A & \gamma_{a-2}^A & \gamma_{a-1}^A \\ \gamma_2^A & \gamma_3^A & \cdots & \gamma_a^A & \gamma_3^A & \gamma_4^A & \cdots & \gamma_{a-1}^A & \gamma_a^A & \gamma_a^A \end{pmatrix} \tag{17b}
$$

$$
g_{\gamma^B}(h_B, j_B) = \begin{pmatrix} \gamma_1^B & \gamma_1^B & \cdots & \gamma_1^B & \gamma_2^B & \gamma_2^B & \cdots & \gamma_{b-2}^B & \gamma_{b-2}^B & \gamma_{b-1}^B \\ \gamma_2^B & \gamma_3^B & \cdots & \gamma_b^B & \gamma_3^B & \gamma_4^B & \cdots & \gamma_{b-1}^B & \gamma_b^B & \gamma_b^B \end{pmatrix} \tag{17c}
$$

Consequently, there are a total number of $C_c^2 C_a^2 C_b^2$ iterations in IFA for the three-factor model expressed as Equation (13). For each iteration, the sums of squares can be reformulated as:

$$
SS_T^j = \sum_{h_C=1}^{2} \sum_{h_A=1}^{2} \sum_{h_B=1}^{2} \sum_{l=1}^{n} R^2_{g_{\theta^C}(h_C, j_C) g_{\gamma^A}(h_A, j_A) g_{\gamma^B}(h_B, j_B) l} - \frac{R^2_{g_{\theta^C}(o, j_C) g_{\gamma^A}(o, j_A) g_{\gamma^B}(o, j_B)}}{8n} \tag{18a}
$$

$$
SS_{\theta^C}^j = \frac{1}{4n} \sum_{h_C=1}^{2} R^2_{g_{\theta^C}(h_C, j_C) g_{\gamma^A}(o, j_A) g_{\gamma^B}(o, j_B)} - \frac{R^2_{g_{\theta^C}(o, j_C) g_{\gamma^A}(o, j_A) g_{\gamma^B}(o, j_B)}}{8n} \tag{18b}
$$

16

$$SS_{\gamma^A}^j = \frac{1}{4n} \sum_{h_A=1}^{2} R^2_{g_{\theta C}(h_C,o)g_{\gamma A}(h_A,j_A)g_{\gamma B}(o,j_B).} - \frac{R^2_{g_{\theta C}(o,j_C)g_{\gamma A}(o,j_A)g_{\gamma B}(o,j_B).}}{8n} \qquad (18c)$$

$$SS_{\gamma^B}^j = \frac{1}{4n} \sum_{h_B=1}^{2} R^2_{g_{\theta C}(h_C,o)g_{\gamma A}(o,j_A)g_{\gamma B}(h_B,j_B).} - \frac{R^2_{g_{\theta C}(o,j_C)g_{\gamma A}(o,j_A)g_{\gamma B}(o,j_B).}}{8n} \qquad (18d)$$

$$SS_e^j = \sum_{h_C=1}^{2}\sum_{h_A=1}^{2}\sum_{h_B=1}^{2}\sum_{l=1}^{n} R^2_{g_{\theta C}(h_C,j_C)g_{\gamma A}(h_A,j_A)g_{\gamma B}(h_B,j_B)l} - \frac{1}{n}\sum_{h_C=1}^{2}\sum_{h_A=1}^{2}\sum_{h_B=1}^{2} R^2_{g_{\theta C}(h_C,j_C)g_{\gamma A}(h_A,j_A)g_{\gamma B}(h_B,j_B).} \qquad (18e)$$

330 $$SS_I^j = SS_T^j - SS_{\theta^C}^j - SS_{\gamma^A}^j - SS_{\gamma^B}^j - SS_e^j \qquad (18f)$$

where

$$R_{g_{\theta C}(h_C,j_C)g_{\gamma A}(h_A,j_A)g_{\gamma B}(h_B,j_B).} = \sum_{l=1}^{n} R_{g_{\theta C}(h_C,j_C)g_{\gamma A}(h_A,j_A)g_{\gamma B}(h_B,j_B)l}$$

$$R_{g_{\theta C}(h_C,j_C)g_{\gamma A}(o,j_A)g_{\gamma B}(o,j_B).} = \sum_{h_A=1}^{2}\sum_{h_B=1}^{2}\sum_{l=1}^{n} R_{g_{\theta C}(h_C,j_C)g_{\gamma A}(h_A,j_A)g_{\gamma B}(h_B,j_B)l} \cdot$$

335 $$R_{g_{\theta C}(o,j_C)g_{\gamma A}(h_A,j_A)g_{\gamma B}(o,j_B).} = \sum_{h_C=1}^{2}\sum_{h_B=1}^{2}\sum_{l=1}^{n} R_{g_{\theta C}(h_C,j_C)g_{\gamma A}(h_A,j_A)g_{\gamma B}(h_B,j_B)l}$$

$$R_{g_{\theta C}(o,j_C)g_{\gamma A}(o,j_A)g_{\gamma B}(h_B,j_B).} = \sum_{h_C=1}^{2}\sum_{h_A=1}^{2}\sum_{l=1}^{n} R_{g_{\theta C}(h_C,j_C)g_{\gamma A}(h_A,j_A)g_{\gamma B}(h_B,j_B)l}$$

$$R_{g_{\theta C}(o,j_C)g_{\gamma A}(o,j_A)g_{\gamma B}(o,j_B).} = \sum_{h_C=1}^{2}\sum_{h_A=1}^{2}\sum_{h_B=1}^{2}\sum_{l=1}^{n} R_{g_{\theta C}(h_C,j_C)g_{\gamma A}(h_A,j_A)g_{\gamma B}(h_B,j_B)l}$$

Also, for each iteration, the corresponding contributions for each factor can be obtained as:

340 $$\eta_A^j = SS_{\gamma^A}^j \big/ SS_T^j \qquad (19a)$$

$$\eta_B^j = SS_{\gamma^B}^j \big/ SS_T^j \qquad (19b)$$

$$\eta_C^j = SS_{\theta^C}^j \big/ SS_T^j \qquad (19c)$$

$$\eta_e^j = SS_e^j \big/ SS_T^j \tag{19d}$$

$$\eta_I^j = 1 - \eta_A^j - \eta_B^j - \eta_C^j - \eta_e^j \tag{19e}$$

345   Finally, the individual and interactive contributions for those factors can be obtained by averaging the corresponding contributions in all iterations, expressed as:

$$\eta_A = \frac{1}{J}\sum_{j=1}^{J} SS_{\gamma^A}^j \big/ SS_T^j \tag{20a}$$

$$\eta_B = \frac{1}{J}\sum_{j=1}^{J} SS_{\gamma^B}^j \big/ SS_T^j \tag{20b}$$

$$\eta_C = \frac{1}{J}\sum_{j=1}^{J} SS_{\theta^C}^j \big/ SS_T^j \tag{20c}$$

350   $$\eta_e = \frac{1}{J}\sum_{j=1}^{J} SS_e^j \big/ SS_T^j \tag{20d}$$

$$\eta_I = \frac{1}{J}\sum_{j=1}^{J} \eta_I^j \tag{20e}$$

where $J = C_c^2 C_a^2 C_b^2$

3. Applications

355   The proposed IFC approach can be applied to various multivariate risk inference problems. In this study, we will apply IFC for multivariate flood risk inference at the Wei River basin in China. The Weihe River plays a key role in the economic development of western China, and thus is known regionally as the 'Mother River' of the Guanzhong Plain of the southern part of the loess plateau (Song et al. 2007; Zuo et al. 2014; Du et al. 2015, Xu et al., 2016). It

360   originates from the Niaoshu Mountain at an elevation of 3485 m above mean sea level in Weiyuan County of Gansu Province (Du et al. 2015). The Weihe River basin is characterized by a semi-arid and sub-humid continental monsoon climate, resulting in significant temporal-spatial variations in precipitation, with an annual average precipitation of 559 mm (Xu et al., 2016). Furthermore, there is a strong decreasing gradient from south to north, in which the

365   southern region experiences a sub-humid climate with annual precipitation ranging from 800 to 1000 mm, whereas the northern region has a semi-arid climate with annual precipitation ranging from 400 to 700 mm (Xu et al., 2016). Over the entire basin, the mean temperature ranges from 6 to 14 ^{0}C, the annual potential evapotranspiration fluctuates from 660 to 1,600, and the annual actual evapotranspiration is about 500 mm (Du et al. 2015).

370

    Observed daily streamflow data at Xianyang and Zhangjiashan gauging stations were used for hydrologic risk analysis. Figure 2 show the locations of these two gauging stations based on the daily stream flow data, the flood peak applied is defined as the maximum daily flow over a period and the associated flood volume is considered as the cumulative flow during the

375   flood period. In this study, the flood characteristics are obtained based on an annual scale. This means that one flood event is identified in each year. The detailed method to identify the flood peak and the associated flood volume can be found in Yue (2000, 2001). Table 1 shows some descriptive statistical values for the considered variables (peak discharge, Q; hydrograph volume, V), in which 47 and 55 flood events are characterized at the Xianyang

380   and Zhangjiashan station, respectively.

19

Place Figure 2 and Table 1 here

385

4. Results Analysis

4.1. Model Evaluation and Selection

There are a number of potential probabilistic models for modelling individual flood variables

390   and their dependence structures. In this study, five alternative distributions, including gamma,

generalized extreme value (GEV), lognormal (LN), Pearson type III (P III), and log-Pearson

type III (LP III) distributions, are employed to describe the probabilistic features of the

chosen flood variables (i.e. peak and volume). Moreover, goodness-of-fit tests are performed

through the indices of Kolmogorov-Smirnov test (K-S test), root mean square error (RMSE)

395   and Akaike Information Criterion (AIC), to screen the performance of those potential models.

The results are presented in Table 2. The results indicate that all five parametric distributions

can produce satisfactory results, with all p-values larger than 0.05. However, it can be

concluded that the GEV and lognormal approaches show the best performance for

respectively modelling flood peak and volume at both gauging stations.

400

Place Tables 2 here

----

405   In addition, a total number of six copulas, including Gaussian, Student t, Clayton, Gumbel,

Frank and Joe copulas, are considered as the candidate models for quantifying the

20

dependence structures for flood peak-volume at Xianyang and Zhangjiashan gauging stations. Also, the goodness-of-fit statistic test is performed based on the Cramér von Mises statistic proposed by Genest et al. (2009). The indices of RMSE and AIC were employed to evaluate the performance of the obtained copulas and identify the most appropriate ones. Table 3 shows statistical test results for the selected copulas. The results show that, for the Zhangjiashan station, all candidate copulas except the Joe copula performed well, while all six copulas would be able to provide satisfactory risk inferences at the Xianyang station. Moreover, based on the values of RMSE and AIC, the Gumbel copula was chosen to model the dependence of flood peak and volume at Zhangjiashan station, while the Joe copulas performed best at the Xianyang station, except that although the p-value is slightly lower than Gumbel, the overall result favours Joe. Consequently, the Gumbel and Joe copula were chosen in this study to further characterize the uncertainty in model parameters and the resulting risks at Zhangjiashan and Xianyang station, respectively.

Place Tables 3 here

4.2. Uncertainty in Model Parameters and Risk Inferences

Based on the results in Tables 2 and 3, the multivariate risk inference model was established, in which the GEV and lognormal distributions would respectively be adopted to model the

430 individual flood variables at both gauging stations, while in comparison, the Gumbel and Joe

copulas would respectively be employed for Zhangjiashan and Xianyang stations. Afterward,

uncertainties would be characterized based on the bootstrap algorithm illustrated in Section

2.3. In this study, a total number of 5000 samples were chosen in order to generally visualize

the uncertainty features in the model parameters. The probabilistic features for obtained

435 parameters values (i.e. shape, scale and location for GEV, meanlog, sdlog for LN, and theta

for copula) for each sample scenario would be described by the kernel method. Figure 3

exhibits the probabilistic distributions for the six unknow parameters in the established

multivariate risk inference model. Extensive uncertainties exist in the parameters for both the

marginal distribution and dependence model. As presented in Figure 3, each parameter,

440 except the meanlog in the LN distribution, exhibits noticeable uncertainty. Moreover, most of

the parameter uncertainties are approximately normally distributed except the shape

parameter in GEV for Xianyang.

----

445 Place Figure 3 here

It is quite apparent that different parameter values in the copula model would lead to different

risk inference results. Consequently, parameter uncertainties in the marginal distributions and

450 copula functions would definitely result in uncertainties in multivariate risk inferences. Based

on the copula model, some multivariate risk indices can be easily obtained, such as the joint

return period in OR, AND and Kendall, as expressed in Equations (12a) – (12c). However,

due to parameter uncertainties, these risk indices may also exhibit some degrees of uncertainty. Figures 4 – 6 describe uncertainties for the joint RP in AND, OR and Kendall at the two stations. In general, the predictive RP in AND exhibit most significant uncertainty, followed by the predictive RP in OR and Kendall. However, for moderate or large flood events, considerable uncertainties can be observed in the inferences for all the three joint RPs. Specifically, noticeable uncertainties exist in the predictive joint RP of AND even for a minor flood event with a 5-year joint RP. For some large flood events with a joint RP around 100 years, the predictive RP in AND shows remarkable uncertainty, ranging from less than 50 years to larger than 200 years. For the joint RP in OR and Kendall, slight uncertainty may exist for small flood events (e.g. 2-year or 5-year joint RP). Nevertheless, apparently uncertainties can be observed in the predictive joint RP even for moderate flood events. As shown in Figure 5, considerable uncertainties may appear in the predictive joint RP of OR even for a flood with an actual joint RP of 20 years, while prediction of the Kendall RP for a 20-year (in Kendall RP) flood event may range from 10 to 50 years, as presented in Figure 6.

Place Figures 4-6 here

4.3 Individual and Interactive Effects of Parameter Uncertainties

It has been observed that parameter uncertainties in the copula-based multivariate risk model would lead to significantly imprecise risk predictions. However, one critical issue to be addressed is how the parameter uncertainties and their interactions would influence the risk

23

inference. Consequently, a multilevel factorial analysis, based on Equations (13) and (14), were proposed to primarily visualize the individual and interactive effects of parameter uncertainties in the marginal and dependence models on the resulting risk inferences. In this study, a total number of 6 parameters (i.e. three from GEV, two from LN, and one from copula) was addresses, and based on probabilistic features of these parameters, three quantile levels (i.e. 0.1, 0.5 and 0.9) were chosen to characterize the resulting risk inferences under different parameter values. This would finally form a 3^6 factorial design, which has six factors with each having three levels. The failure probability denoted as Equations (11) would be considered as the response in this factorial design.

The main and interactive effects of parameters uncertainties on the failure probabilities in AND are visualized in Figure 7. It is noticeable that at the two gauge stations, parameters uncertainties pose similar main and interactive effects on the failure probabilities in AND, which indicates that parameters' effects (individual and interactive) on the failure probability in AND are independent of the location of gauge stations. More specifically, variations in the shape parameter in GEV and *sdlog* parameter in LN would lead to more changes in the corresponding responses (i.e. failure probability in AND) than the variations in other parameters. Also, as shown in Figure 7, the parameter in the copula function (i.e. Cop_theta), describing dependence of the two flood variables, would not have an effect on the resulting risk as much as the effects from the parameters (except the location parameter in GEV) in the marginal distributions. In terms of parameter interactions, the significance of interactive effects for different parameters varies. The interactive curves for some parameters (e.g. GEV_shape and GEV_location) are nearly parallel at the three levels, indicating an

24

500   insignificant interaction for these two parameters on the inferred risk. In comparison, there

are also some interactive curves intersecting each other (e.g. GEV_shape and LN_meanlog),

implying a significant interaction between these two parameters. Table 4 provides the results

from an ANOVA table for the failure probability in AND. It is quite interesting that: i) even

though the effect from the parameter in the copula function is not as visible as the effects

505   from the parameters (except the location parameter in GEV) in the marginal distributions (as

shown in Figure 7), such an effect is still statistically significant; ii) the effect from the

location parameter of GEV is statistically insignificant, which also lead to insignificant

interactive effects between the location parameter and other parameters; iii) the interactions

between the parameter in copula and the parameters in marginal distributions would be more

510   likely statistically insignificant; iv) the statistical significance (significant or not) for

individual and interactive effects from parameters is almost the same between these two

gauge stations. All these conclusions obtained from Table 4 are consistent with the

implications described in Figure 7.

515   --------------------------------

Place Figures 7 and Table 4 here

In terms of the failure probabilities in OR and Kendall, as presented in Figures 8 and 9, these

520   have similar patterns with the failure probability in AND (presented in Figure 7). The

individual/main effects from the marginal distributions (except the location parameter in

GEV) are generally more visible than the parameters in copula functions. Also, some

interactive curves, especially the curves between GEV_location and others, are parallel, showing insignificant interaction between those parameters. More detailed characterizations

525 of the main and interactive effects for the failure probabilities in OR and Kendall are described in the ANOVA tables in Tables 5 and 6. These two tables show some slight differences from the conclusions given by Table 4. The location parameter in GEV also has a statistically significant effect on the failure probabilities results in OR and Kendall, which also leads to some significant interactions between this parameter and other model

530 parameters. For the failure probability in Kendall, the parameter in the copula would have more interactions with other parameters in marginal distributions than the interactions in the failure probability in AND and OR. As presented in Table 6, the parameter in the copula would have a statistically significant effect on the inferred failure probability in Kendall with other parameters except the location parameter in GEV. These results are also implied in the

535 main effects plots and full interactions plot matrices in Figures 8 and 9.

\---

Place Figures 8-9 and Table 5 - 6 here

\---

540

Based on the three-level factorial analysis, it can be generally concluded that the parameters in the marginal distributions (except the location parameter in GEV) would have more individual effects on joint risk inference than the parameter in the copula. The risk indices (i.e. AND, OR, or Kendall) would not have significantly influenced the individual effects of

545 model parameters. However, for the interactive effects among model parameters, they may

26

exhibit slightly different patterns. Specifically, the parameter in the copula would have more significant interactions with parameters in the marginal distributions on the failure risk in Kendall than the other two risk indices. Moreover, the individual and interactive effects from the model parameters on risk inferences would not be influenced by the location of the gauge stations.

4.4. Contribution Partition of Uncertainty Sources

As a result of parameter uncertainties, the predictive failure probabilities exhibit noticeable uncertainties, as shown in Figures 4-6. The three-level factorial analysis based on Equations (11) is able to provide a primary description and visualization related to the individual and interactive effects of parameter uncertainty on the inferred failure probabilities. However, two critical issues to be answered are: (i) how much would parameter uncertainties contribute to the variation of the inferred risk values? and (ii) do these contributions change significantly for failure probabilities with different service time scenarios? To address these two issues and get reliable results, an iterative factorial approach (IFA) has been proposed, which is formulated as Equations (16) – (20). Also, like the three-level factorial analysis, three quantile levels were selected at 0.1, 0.5, and 0.9. Based on IFA, each parameter at its three quantile values (0.1, 0.5, 0.9) would be further subsampled into three scenarios of two quantile values (i.e. (0.1, 0.5), (0.1, 0.9), and (0.5, 0.9)). For this study, we have a total number of 6 parameters with each having three quantile values at 0.1, 0.5, and 0.9, which would lead to a total number of 729 (i.e. 3^6) two-level factorial designs.

Figure 10 shows the detailed contribution table of the model parameters on uncertainty in

570   predictive failure probabilities of AND at the two gauge stations. It can be observed that,

even though some discrepancies exist at Zhangjiashan and Xingshan stations, the detailed

contributions for each parameter and their interaction show quite similar features between

these two stations. In detail, uncertainty in the shape parameter in GEV has the most

significant impact on the failure probability in AND, followed by *sdlog* in LN, parameter

575   interaction, *meanlog* in LN, and *scale parameter* in GEV. Moreover, the uncertainty in the

parameter in the copula would not lead to a significant variation in the resulting failure

probability predictions in AND, which merely makes a contribution less than 0.5%. Such

conclusions are also generally consistent with the ANOVA results presented in Figure 7 and

Table 4. Furthermore, with the increase in service time, the contributions of each parameter

580   and their interactions do not vary significantly. Some individual contributions from parameter

uncertainties would slightly increase while other individual contributions may slightly

decrease. However, the effect from parameter interactions would generally increase with the

increase of service time. In comparison, the enhancement in design standards for hydraulic

infrastructures would lead to a greater chance for deceases in individual effects and, at the

585   same time, increases in parameter interactions. For instance, as the flood design standard

increases from 200-year to 500-year for a hydraulic facility with 30-year service time near the

Zhangjishan station, the interactive effect of model parameters would increase from 15.14%

to 18.09%.

590   ---

Place Figure 10 here

In terms of the failure probability in OR, the individual and interactive effects of model

595   parameters on predictive risk uncertainties show similar ==patterns== with the parameters' effects

on the failure probability in AND. As shown in Figure 11, the *shape parameter* in the GEV

distribution and the *sdlog* in the LN distribution are the two major ==sources of uncertainty== in

failure probabilities in OR. However, compared with the failure probability in AND,

parameter interaction has a less effect on the resulting uncertainty of risk inference in OR. As

600   shown in Figures 10 and 11, the effect of parameter interaction on the risk in AND ranges

between 13.96% and 20.05%, while in comparison, the parameters' interactive effect on the

risk in OR varies ==between 10.25% and 11.57%.== Apparently, it can also be observed that some

external factors such as the design standard and service time of hydraulic infrastructures have

less influence on the parameters' interaction on risk in OR than the risk in AND. However,

605   the first contributor (i.e. shape parameter in GEV) would have a ==larger== contribution on the

predictive uncertainty in the failure probability in OR as the increase in the design standard,

while in comparison, this contributor would have a ==lower== contribution on the risk in AND.

For instance, as the design return period of flood (i.e. design standard) increases from 200 to

500 years and the service time of the hydraulic facility is 30 years, the contribution of the

610   shape parameter in GEV would increase from 47.62% to 50.64% for the failure probability in

OR at the Xianyang station, while the parameter's contribution on the failure probability in

AND decreases from 49.26% to 45.77%.

----

615   Place Figure 11 here

        For the failure probability in Kendall, the contributions of model parameters and their

        interaction are presented in Figure 12. Similar to the failure probabilities in AND and OR, the

620   *shape parameter* in the GEV distribution and the *sdlog* parameter in the LN distribution are

        the two major contributors, which can account for nearly 70% or more in the predictive

        uncertainty of the failure probability in Kendall. Meanwhile, the *scale parameter* in GEV,

        meanlog in LN, and parameters' interaction also have noticeable effects on the risk in

        Kendall, ranging from 4.72% (*scale parameter* in GEV) to 12.64% (*meanlog* in LN).

625   Conversely, the *location parameter* in GEV and the dependence parameter in copula merely

        have relatively minor individual effects. However, it is noticeable that, although the

        dependence parameter has a minor effect (0.78%, 1.03%) on the risk in Kendall, such an

        effect is much higher than the effect on the risk in AND (less than 0.23%) and the risk in OR

        (less than 0.06%).

630

        Place Figure 12 here

        ----

635   Even through the prediction equations for the failure probabilities in AND, OR and Kendall,

        as presented in Equations (12) are different, the impacts of parameter uncertainties show

        quite similar features, in which the *shape parameter* in GEV and the *sdlog* in LN are the two

major contributors to the predictive uncertainties in risk inferences. Nearly 70% and more variability in the uncertainties in risk inferences can be attributed by the uncertainties in the

640   *shape parameter* in GEV and *sdlog* parameter in LN. Also some external factors such as flood design and facility service time may have different influences on parameters' effects for different risk indices, such influences are not significant and would not lead to remarkable changes in parameters' contribution to risk inferences. Parameters' interaction has a greater effect on risk inference in AND than the other two risk indices (i.e. OR, Kendall), while the

645   contribution from the dependence parameter, even though not noteworthy, has a larger effect on the risk inference in Kendall.

5. Discussion

5.1. Differences for the Hydrologic Risk Models at Different Stations

650

Different copula functions are applied for different stations, which are chosen based on the indices of RMSE and AIC. However, the selection of copula models at different stations may also be related with some key characteristics of the drainage areas for those stations. The Gumbel copula will be applied for the Zhangjiashan station. It can reflect strong correlation

655   at high values. However, the Joe copula, which is adopted at the Xianyang station, can reflect a stronger right tail positive dependence than Gumbel copula. Both the Xianyang and Zhangjiashan stations have similar drainage areas. The Xianyang station controls a drainage area of 46,480 km^2 (Xu et al., 2016), while the Zhangjiashan station has a drainage area of 45,412 km^2 (Sun et al., 2019). Nevertheless, the major reason that lead to different copula

660 functions at these two stations may be due to the elevation features for those two drainage areas. The drainage area of Zhangjiashan station is located in the central part of Loess Plateau of China, which is mainly characterized as a mountainous region. In comparison, even though a large part of the drainage area of Xianyang station is also located in the mountainous region, the Xianyang station also controls a large part of the Guanzhong Plain, as indicated in

665 the red part of Figure 2. Consequently, the flood hydrograph at Zhangjiashan station may be sharp while the flood hydrograph at Xianyang station is relatively flat and show a stronger right tail dependence among flood peak and volume. In fact, the value of Kendall's tau between peak and volume for the top ten floods at Zhangjiashan station is 0.33 while such a value of Kendall's tau at Xianyang station is 0.6. These facts may explain that the Gumbel

670 copula is applicable for Zhangjiashan station while the Joe copula is applied for Xianyang station. However, this is an initial guess and may need to be further demonstrated through more cases in different areas.

5.2. Contribution Partition of Uncertainty Sources through Different Approaches

675

In this study, the individual and interactive contributions of parameter uncertainties are quantified through the developed IFA approach, in which each parameter has three levels (i.e. 0.1, 0.5, 0.9 quantiles) to be subsampled. In fact, the parameters' contributions can also be characterized by the traditional factorial analysis (FA) approach based on Equations (15) as

680 well as the IFA approach with more factor levels (e.g. 4 or 5 levels for each parameter).

Figure 13 shows the comparison of parameter contributions to predictive uncertainty for

32

failure probabilities in AND at the Zhangjiashan station for three and four parameter levels scenarios for the design standard of 200-year. The results of Figure 13(b) are obtained

685   through the IFA approach with each parameter having four levels to be its quantiles at 0.1, 0.35, 0.6, 0.85. Also, Table 7 presents the parameter contributions to predictive uncertainty in failure probabilities obtained by traditional FA approach for Zhangjiashan stations with the design standard of 200-year and service time of 30-year.

----

690   Place Figure 13 and Table 7 here

It can be seen that for different subsampling scenarios, the resulting contributions may be different. However, such a difference would be tolerable since (1) the variations of

695   parameters' contributions are relatively small and mainly happen for the first two contributors, (2) the total contribution of the first two contributors does not change remarkably (around 70% in total), (3) the contributions of other factors especially the parameters' interaction do not vary significantly, and (4) the rank of the contributions from different sources does not change for the two subsampling scenarios. In comparison, as

700   presented in Table 7, the contribution partition of parameter uncertainties obtained through traditional FA shows totally different patterns for different risk inferences. Specifically, the traditional FA approach would significantly overestimate parameter interactive effects on risk inference in AND, at the same time, underestimate the interactive effects on risk inference in OR and Kendall. Consequently, the contribution rank of parameter uncertainties from

705   traditional FA is different from the results obtained through the developed IFA approach.

33

As shown in Figure 13, the proposed IFA approach may lead to slightly different results for different subsampling schemes (four or five levels). However, an increase in parameter level would highly increase computational demand. For instance, if each parameter has four levels, the IFA approach would lead to a total number of 46,656 (i.e. 6^6) two-level factorial designs. Moreover, the subsampling scheme for factors with five levels would lead to a total number of one million (i.e. 10^6) two-level factorial designs. Consequently, the three-level subsampling scheme would generally be recommended and also can generate acceptable results.

5.3. Correlation among Parameters' Contributions

The proposed IFA approach would generally produce a great number of two-level factorial designs. For one specific factor (e.g. *GEV_shape*), it would have two levels (lower and upper levels) for all factorial designs. However, the detailed value for the lower or upper level may be different in different factorial designs. This may finally lead to different contributions for this factor. Figure 14 presents the variations of parameters' contributions to the prediction of failure probabilities in AND, OR, and Kendall. We already concluded that the shape parameter in GEV (i.e. *GEV_shape*) and the *sdlog* in LN (i.e. *LN_sdlog*) distribution would generally have the most significant contributions to predictive uncertainties in risk inferences. However, as shown in Figure 14, the detailed contributions for these two parameters would vary remarkably for different level values in different factorial designs. In comparison, the contributions from other parameters and their interaction have less fluctuation than the

individual contributions of *GEV_shape* and *LN_sdlog*. For instance, although the *meanlog* in

730   LN (i.e. *LN_meanlog*), with an average contribution of more than 10%, may have some

chance to pose a predominant contribution of more than 50%, most of its contribution is

positively distributed within [0, 25%]. Also, even though the parameters' interaction has a

noteworthy average contribution larger than 10%, all the detailed contributions in different

factorial designs are located within [0, 25%].

735

Place Figure 14 here

----

740   It has been observed that the parameters' contribution may vary significantly due to the

differences in factor values in different factorial designs. One potential issue to be addressed

is that how those individual and interactive contributions correlate with each other. Figure 15

presents the Pearson's correlation among individual and interactive contributions of model

parameters to different risk inferences (i.e. failure probabilities in AND, OR, and Kendall). It

745   is noticeable that the parameters in the LN distribution (i.e. *LN_sdlog*, *LN_meanlog*) are

generally negatively correlated with the parameters in the GEV distribution (i.e. *GEV_shape*,

GEV_scale, and *GEV_location*). Also, for one marginal distribution (LN or GEV), its

parameters are positively correlated. This implies that an increase in the contribution of one

parameter would lead to a contribution increase for parameters within the same distribution

750   and at the same time result in a contribution decrease for all parameters in the other

distribution. Moreover, if statistically significant, the contribution of the dependent parameter

(i.e. parameter in copula) generally has positive correlation with the contributions from other parameters except GEV_shape and parameters' interaction. Also, the contributions from parameters' interactions are generally negatively correlated with the individual contributions from other parameters if such correlation is statistically significant.

Place Figure 15 here

The proposed IFA approach can generally characterize how parameter uncertainties would influence the predictive uncertainties in risk inferences. A large number of two-level factorial designs were produced due to different subsampling procedures and then used to generate different partition results for parameters' contributions. However, for different risk inferences (i.e. failure probabilities in AND, OR, and Kendall), these partition results have similar variation features and also show similar correlation plots.

6. Conclusions

Uncertainty quantification is an essential issue for both univariate and multivariate hydrological risk analyses. A number of research works have been posed to reveal uncertain features in multivariate hydrological risk inference. However, it is required to know the major sources/contributors for predictive uncertainties in multivariate risk inferences. In this study, an iterative factorial copula approach (IFC) has been proposed for uncertainty quantification

775 and partition in multivariate hydrologic risk inference. In IFC, a copula-based multivariate

risk model has been developed and the bootstrap method is adopted to quantify the

probabilistic features for the parameters in both marginal distributions and the dependence

model. An iterative factorial analysis (IFA) approach is finally developed to diminish the

effect of the sample size in traditional ANOVA computation and provided reliable

780 contribution partition for parameter uncertainties in different risk inferences.

The proposed method has been applied for flood risk inferences at two gauge stations in Wei

River basin. The results indicate that uncertainties in the parameters of the copula-based

model would lead to noticeable uncertainties in the resulting risk inferences, especially for

785 the joint flood risk in AND. noticeable uncertainties exist in the predictive joint RP of AND

even for a small flood event. However, the results from IFA suggested that those uncertainties

in risk inferences may mainly be attributed to the uncertainties in *shape parameter* in GEV

distribution and the parameter of *sdlog* in LN for both the two stations. In comparison, the

parameter uncertainty in the copula function would not pose an obvious effect on the

790 resulting uncertainty in risk inferences. Such results indicate that, at least that the Wei River

basin, the decision makers need to well estimate the values or quantify the uncertainties for

the *shape parameter* in GEV distribution and *sdlog* in the LN distribution, in order to obtain

reliable risk inferences. For other catchments, the proposed IFC method can be adopted to

reveal the major sources for uncertainties in risk inferences and then provide potential

795 pathways to get reliable risk inferences.

This study is the first attempt to characterize parameter uncertainties in a copula-based

multivariate hydrological risk model and further reveal their contributions to predictive uncertainties for different risk inferences. As an improvement of ANOVA, the developed IFA

800   method can mitigate the effect of bias variance estimation in ANOVA and generate reliable results. Moreover, another noteworthy feature for the IFA approach is that it does not only characterize the impacts for continuous factors (e.g. model parameters in this study), but also reveals the impacts of discrete or non-numeric factors. Such a feature can allow the proposed IFA approach to be employed to further explore the impacts of non-numeric factors (e.g.

805   model structures, sample size) in hydrologic systems analysis.

References

Bobee, B., Cavidas, G., Ashkar, F., Bernier, J., Rasmussen, P.: Towards a systematic approach to comparing distributions used in flood frequency analysis, J. Hydrol., 142, 121–136, 1993.

Bosshard, T., Carambia M., Georgen K., Kotlarski S., Krahe P., Zappa M., Schar C.,: Quantifying uncertainty sources in an ensemble of hydrological climate-impact projections. Water Resour. Res., 49(3): 1523-1536, DOI:10.1029/2011wr011533, 2013.

Chebana F., and Ouarda T.B.M.,: Multivariate quantiles in hydrological frequency analysis. Environmetrics, 22(1), 63-78, 2011.

Cunnane, C.: Statistical distributions for flood frequency analysis. Operational Hydrological Report, No. 5/33, World Meteorological Organization (WMO), Geneva, Switzerland, 1989.

De Michele C, Salvadori G.: A Generalized Pareto intensity-duration model of storm rainfall exploiting 2-copulas. J. Geophys. Res., 108(D2), 4067, doi:10.1029/2002JD002534, 2003.

Dung N.V., Merz B., Bardossy A., Apel H.:. Handling uncertainty in bivariate quantile estimation – An application to flood hazard analysis in the Mekong Delta. J. Hydrol., 527, 704-717, 2015.

Du T, Xiong L, Xu CY, Gippel CJ, Guo S, Liu P.: Return period and risk analysis of nonstationary low-flow series under climate change. J. Hydrol., 527, 234-250, 2015.

Fan Y.R., Huang K., Huang G.H., Li Y.P.,: A factorial Bayesian copula framework for partitioning uncertainties in multivariate risk inference. Environ. Res., 183, 109215, 2020.

Fan Y.R., Huang W.W., Huang G.H., Huang K., Zhou X.,: A PCM-based stochastic hydrologic model for uncertainty quantification in watershed systems. Stochastic Environ. Res. Risk Assess., 29(3) 915-927, 2015a.

Fan Y.R., Huang W.W., Li Y.P., Huang G.H., Huang K.: A coupled ensemble filtering and probabilistic collocation approach for uncertainty quantification of hydrological models. J. Hydrol., 530, 255-272, 2015b.

850 Fan Y.R., Huang W.W., Huang G.H., Huang K., Li Y.P., Kong X.M.: Bivariate hydrologic risk analysis based on a coupled entropy-copula method for the Xiangxi River in the Three Gorges Reservoir area, China, Theor. Appl. Climatol., 125 (1-2), 381-397, doi:10.1007/s00704-015-1505-z, 2016a

Fan Y.R., Huang W.W., Huang G.H., Li Y.P., Huang K.: Hydrologic Risk Analysis in the Yangtze River basin through Coupling Gaussian Mixtures into Copulas. Adv. Water Resour., 88, 170-185, 2016b.

Fan Y.R., Huang G.H., Baetz B.W., Li Y.P., Huang K.,: Development of a Copula‐based Particle Filter

855 (CopPF) Approach for Hydrologic Data Assimilation under Consideration of Parameter Interdependence. Water Resour. Res., 53(6), 4850-4875, 2017.

Fan Y.R., Huang G.H., Zhang Y., Li Y.P.,: Uncertainty quantification for multivariate eco-hydrological risk in the Xiangxi River within the Three Gorges Reservoir Area in China, Engineering 4 (5), 617-626, 2018.

860 Genest C, Rémillard B, Beaudoin D.: Goodness-of-fit tests for copulas: A review and a power study. Insurance: Mathematics and Economics, 44:199-213, 2009.

Graler B., van den Berg M.J., Vandenberghe S., Petroselli A., Grimaldi S., De Baets B., Verhoest N.E.C.,:

Multivariate return periods in hydrology: a critical and practical review focusing on synthetic design

hydrograph estimation. Hydrol. Earth Syst. Sci. 17: 1281–1296, 2013.

865 Huang K., Dai L.M., Yao M., Fan Y.R., Kong X.M.: Modelling dependence between traffic noise and traffic flow through an entropy-copula method, J. Environ. Inform., 29(2) 134-151, doi:10.3808/jei.201500302, 2017.

Kao S.C., Govindaraju R.S.: A copula-based joint deficit index for droughts. J. Hydrol., 380, 121-134, 2010.

870 Karmakar S., Simonovic S.P.: Bivariate flood frequency analysis. Part 2: a copula-based approach with mixed marginal distributions. J. Flood Risk Manage., 2, 32-44, 2009.

Kidson R., Richards K.S.: Flood frequency analysis: assumption and alternatives. Prog. Phys. Geogr., 29(3), 392-410, 2005.

Kong X.M., Zeng X.T., Chen C., Fan Y.R., Huang G.H., Li Y.P., Wang C.X.: Development of a Maximum

875   Entropy-Archimedean Copula-Based Bayesian Network Method for Streamflow Frequency Analysis—
A Case Study of the Kaidu River Basin, China, Water, 11(1), 42, 2019

Kong X.M., Huang G.H., Fan Y.R., Li Y.P.: Maximum entropy-Gumbel-Hougaard copula method for simulation of monthly streamflow in Xiangxi river, China. Stochastic Environ. Res. Risk Assess., 29, 833-846, 2015

880   Lee T, Salas JD.: Copula-based stochastic simulation of hydrological data applied to Nile River flows. Hydrol. Res. 42(4): 318–330, 2011.

Ma M., Song S., Ren L., Jiang S., Song J.: Multivariate drought characteristics using trivariate Gaussian and Student copula. Hydrol. Processes, 27, 1175-1190, 2013.

Merz B, Thieken A.H.: Separating natural and epistemic uncertainty in flood frequency analysis. J.

885   Hydrol., 309(1–4):114–132, 2005.

Montgomery, D. C. (Eds.). Design and analysis of experiments (5th ed.). New York: John Wiley & Sons Inc., 2001.

Nelsen R.B., (Eds.). An Introduction to Copulas. Springer: New York, 2006.

Qi, W., Zhang, C., Fu, G., Zhou, H.: Imprecise probabilistic estimation of design floods with epistemic

890   uncertainties. Water Resour. Res., 52(6), 4823–4844, doi:10.1002/2015WR017663, 2016a.

Qi, W., Zhang, C., Fu, G., Zhou, H.: Quantifying dynamic sensitivity of optimization algorithm parameters to improve hydrological model calibration. J. Hydrol., 533: 213-223, DOI:10.1016/j.jhydrol.2015.11.052, 2016b

Requena A., Mediero L., Garrote L.: A bivariate return period based on copulas for hydrologic dam design:

895   Accounting for reservoir routing in risk estimation. Hydrol. Earth Syst. Sci. 17(8):3023-3038, 2013.

Reddy M.J., Ganguli P.: Bivariate flood frequency analysis of Upper Godavari River flows using

Archimedean copulas. Water Resour. Manage. 26 (14), 3995-4018, 2012

Sadegh M., Ragno E., AghaKouchak, A.: Multivariate Copula Analysis Toolbox (MvCAT): Describing

dependence and underlying uncertainty using a Bayesian framework, Water Resour. Res., 53, 5166–

900   5183, doi:10.1002/ 2016WR020242, 2017

Salvadori G., De Michele C., Durante F.: On the return period and design in a multivariate framework.

Hydrol. Earth Syst. Sci. 15: 3293–3305, 2011

Salvadori, G., F. Durante, C. De Michele, M. Bernardi, and L. Petrella: A multivariate copula-based

framework for dealing with hazard scenarios and failure probabilities, Water Resour. Res., 52, 3701–

905   3721, doi:10.1002/2015WR017225, 2016

Salvadori G., De Michele C., Kottegoda N.T., Rosso R., (Eds.). Extremes in Nature: an Approach using

Copula. Springer: Dordrencht; 2007.

Sarhadi, A., D. H. Burn, M. C. Ausín, and M. P. Wiper: Time-varying nonstationary multivariate risk

analysis using a dynamic Bayesian copula, Water Resour. Res., 52, 2327–2349,

910   doi:10.1002/2015WR01852, 2016

Song J, Xu Z, Liu C, Li H.: Ecological and environmental instream flow requirements for the Wei River –
the largest tributary of the Yellow River. Hydrol. Processes, 21, 1066-1073, 2007

Song S., Singh V.P.: Meta-elliptical copulas for drought frequency analysis of periodic hydrologic data.

Stochastic Environ. Res. Risk Assess., 24(3), 425-444, 2010.

915   Sraj M., Bezak N., Brilly M.: Bivariate flood frequency analysis using the copula function: a case study of

the Litija station on the Sava River. Hydrol. Processes, 29(2), 225-238, 2014.

Sun C.X., Huang G.H., Fan Y.R., Zhou X., Lu C., Wang X.W.: Drought occurring with hot extremes:

Changes under future climate change on Loess Plateau, China, Earth's Future, 7(6), 587-604, 2019.

The European Parliament and The Council: Directive 2007/60/EC: On the assessment and management of flood risks, Official Journal of the European Union, 116 pp, 2007

Vandenberghe S, Verhoest NEC, De Baets B.: Fitting bivariate copulas to the dependence structure between storm characteristics: a detailed analysis based on 105 year 10 min rainfall. Water Resour. Res., 46. DOI: 10.1029/2009wr007857, 2010.

Xu Y., Huang G.H., Fan Y.R.: Multivariate flood risk analysis for Wei River. Stochastic Environ. Res. Risk Assess., 31 (1), 225-242 doi: 10.1007/s00477-015-1196-0, 2016

Yue S.: The bivariate lognormal distribution to model a multivariate flood episode. Hydrol. Processes, 14(14), 2575-2588, 2000

Yue S.: A bivariate gamma distribution for use in multivariate flood frequency analysis. Hydrol. Processes, 15(6), 1033-1045, 2001

Zhang L, Singh VP: Bivariate rainfall frequency distributions using Archimedean copulas. J. Hydrol., 332(1–2):93–109, 2007.

Zhang Q., Xiao M.Z., Singh V.P.: Uncertainty evaluation of copula analysis of hydrological droughts in the East River basin, China. Global Planet. Change, 129, 1-9, 2015.

Captions of Tables

Table 1. Flood characteristics for different stations

Table 2. Statistical test results for marginal distribution estimation: LN means lognormal distribution, P III means Pearson Type III distribution, and LP III means log-Pearson Type III distribution. K-S test denotes the Kolmogorov–Smirnov test.

Table 3. Performance for quantifying the joint distributions between flood peak and volume through different copulas: CvM is the Cramér von Mises statistic proposed by Genest et al. (2009), with p-value larger than 0.05 indicating satisfactory performance.Table 4. Statistical test results for marginal distribution estimation

Table 4. ANOVA table for failure probability in AND: A indicates the shape parameter in GEV, B indicates the scale parameter of GEV, C indicates the location parameter of GEV, D means the meanlog of LN, E means the sdlog of LN, and F mean the parameters (i.e. theta) in copula Comparison of RMSE and AIC values for joint distributions through different copulas

Table 5. ANOVA table for failure probability in OR: A indicates the shape parameter in GEV, B indicates the scale parameter of GEV, C indicates the location parameter of GEV, D means the meanlog of LN, E means the sdlog of LN, and F mean the parameters (i.e. theta) in copula

Table 6. ANOVA table for failure probability in Kendall: A indicates the shape parameter in GEV, B indicates the scale parameter of GEV, C indicates the location parameter of GEV, D means the meanlog of LN, E means the sdlog of LN, and F mean the parameters (i.e. theta) in

Table 7. Contributions of parameter uncertainties obtained by three level ANOVA to predictive failure probabilities for a design return period of 200-year and service time of 30-year

Captions of Figures

Figure 1: Framework of the proposed IFC approach

Figure 2. The location of the studied watersheds. Wei River is the largest tributary of Yellow river, with a drainage area of 135,000 km2. The historical flood data from Xianyang and Zhangjiashan stations on the Wei River are analyzed through the proposed IFC approach.

Figure 3. Probabilistic features for parameters in marginal distributions and copula: for both Xianyang and Zhangjiashan stations, the GEV (parameters include shape, scale and location) function would be employed to quantify the distribution of flood peak, while the lognormal distribution (parameters denoted as meanlog and sdlog) is applied for flood volume. The

44

Gumbel and Joe copula (parameter denoted as theta) would be respectively adopted to model the dependence between flood peak and volume at Zhangjiashan and Xianyang stations.

Figure 4. Uncertainty quantification of the joint RP in "AND": the red dash lines indicate the predictive means, the two blue dash lines respectively indicate the 5% and 95% quantiles, and the grey lines indicate the predictions under different parameter samples with the same joint RP of the red and blue dash lines; The cyan lines denote the predictions under different return periods with the model parameters being their mean values.

Figure 5. Uncertainty quantification of the joint RP in "OR": the red dash lines indicate the predictive means, the two blue dash lines respectively indicate the 5% and 95% quantiles, and the grey lines indicate the predictions under different parameter samples with the same joint RP of the red and blue dash lines; The cyan lines denote the predictions under different return periods with the model parameters being their mean values.

Figure 6. Uncertainty quantification of the joint RP in "Kendall": the red dash lines indicate the predictive means, the two blue dash lines respectively indicate the 5% and 95% quantiles, and the grey lines indicate the predictions under different parameter samples with the same joint RP of the red and blue dash lines; The cyan lines denote the predictions under different return periods with the model parameters being their mean values

Figure 7. Main effects plot and full interactions plot matrix for parameters on the failure probability in AND at the two gauge stations

Figure 8. Main effects plot and full interactions plot matrix for parameters on the failure probability in OR at the two gauge stations

Figure 9. Main effects plot and full interactions plot matrix for parameters on the failure probability in Kendall at the two gauge stations

Figure 10. Contributions of parameter uncertainties to predictive failure probabilities in AND under different design standards (i.e. return periods (RP)) and different service periods

Figure 11. Contributions of parameter uncertainties to predictive failure probabilities in OR under different design standards (i.e. return periods (RP)) and different service periods

Figure 12. Contributions of parameter uncertainties to predictive failure probabilities in Kendall under different design standards (i.e. return periods (RP)) and different service periods

Figure 13. Comparison of parameter contributions to predictive uncertainty for failure probabilities under different levels of subsampling for Zhangjiashan station: three (i.e. 0.1, 0.5, 0.9) and four (i.e. 0.1, 0.35, 0.6, 0.85) level quantiles are adopted for subsampling and the design return period is 200 years.

Figure 14. Variation of parameters' contributions for different risk inferences at the Zhangjiashan Station for a design standard of 200-year and a service time of 30-year

Figure 15. Correlation for parameters' contributions on risk inferences at Zhangjiashan station for a design standard of 200-year and a service time of 30-year: The cross sign indicates the correlation is statistically insignificant

1005

Table 1. Flood characteristics for different stations

Station name	period		flood variable	
			Peak (m^3/s)	Volume (m^3/(s day))
		Minimum	139	317
Xianyang	1960-2006	Median	1350	2491
		Maximum	12380	17802
		Minimum	217	303.7
Zhangjiashan	1958-2012	Median	775	1365.3
		Maximum	3730	7576.1

Table 2. Statistical test results for marginal distribution estimation: LN means lognormal distribution, P III means Pearson Type III distribution, and LP III means log-Pearson Type III distribution. K-S test denotes the Kolmogorov–Smirnov test.

Station name	Flooding variables	Marginal distribution	K-S test		RMSE	AIC
			T	P-value		
Zhangjiashan	Peak	Gamma	0.0745	0.5471	0.0378	-323.5512
		GEV	**0.0724**	**0.9151**	**0.0275**	**-389.3956**
		LN	0.0805	0.8403	0.0283	-388.3297
		P III	0.0893	0.7386	0.0395	-349.3274
		LP III	0.0795	0.8508	0.0324	-371.3614
	Volume	Gamma	0.1460	0.1735	0.0596	-306.2925
		GEV	0.1017	0.5839	0.0369	-357.0852
		LN	**0.0904**	**0.7250**	**0.0361**	**-361.3353**
		P III	0.1589	0.1112	0.0737	-280.8701
		LP III	0.0967	0.6468	0.0367	-357.5476
Xianyang	Peak	Gamma	0.1159	0.5533	0.0372	-305.4087
		GEV	**0.0875**	**0.8645**	**0.0305**	**-321.9202**
		LN	0.1051	0.6763	0.0436	-290.5248
		P III	0.1202	0.5051	0.0416	-292.8448
		LP III	0.1321	0.3848	0.0617	-255.8931
	Volume	Gamma	0.1146	0.5305	0.0450	-287.4880
		GEV	0.0540	0.9980	0.0195	-364.3058
		LN	**0.0670**	**0.9749**	**0.0192**	**-367.3885**
		P III	0.1005	0.6913	0.0377	-302.0492
		LP III	0.0722	0.9522	0.0313	-319.6540

Table 3. Performance for quantifying the joint distributions between flood peak and volume through different copulas: CvM is the Cramér von Mises statistic proposed by Genest et al. (2009), with p-value larger than 0.05 indicating satisfactory performance.

		RMSE	AIC	CvM	p-value
Zhangjiashan	Gaussian	0.0669	-295.5144	7.9302	0.7770
	Student t	0.0669	-293.5237	8.5203	0.5976
	Clayton	0.0843	-270.0616	9.4615	0.3290
	Gumbel	**0.0637**	**-300.8577**	**7.9342**	**0.7580**
	Frank	0.0690	-292.0723	9.0704	0.4480
	Joe	0.0606	-306.3185	11.0321	0.0290
Xinshan	Gaussian	0.0513	-277.1704	8.4731	0.2400
	Student t	0.0510	-275.6834	8.2295	0.2885
	Clayton	0.0618	-259.7391	8.2051	0.3240
	Gumbel	0.0477	-283.9933	7.1344	0.6700
	Frank	0.0562	-268.6861	8.2725	0.2940
	Joe	**0.0446**	**-290.2631**	**6.9905**	**0.6540**

Table 4. ANOVA table for failure probability in AND: A indicates the shape parameter in GEV, B indicates the scale parameter of GEV, C indicates the location parameter of GEV, D means the meanlog of LN, E means the sdlog of LN, and F mean the parameters (i.e. theta) in copula

Parameter	Zhangjiashan					Xianyang				
	SS	DF	MS	F-Value	P-value	SS	DF	MS	F-Value	P-value
A	0.37	2	0.18	7512.32	< 0.0001	0.59	2	0.30	5079.77	< 0.0001
B	0.018	2	8.905E-003	362.65	< 0.0001	0.013	2	6.527E-003	111.71	< 0.0001
C	8.313E-005	2	4.156E-005	1.69	**0.1849**	8.642E-005	2	4.321E-005	0.74	**0.4777**
D	0.059	2	0.029	1195.61	< 0.0001	0.082	2	0.041	701.54	< 0.0001
E	0.18	2	0.092	3766.70	< 0.0001	0.31	2	0.16	2656.85	< 0.0001
F	9.379E-004	2	4.690E-004	19.10	< 0.0001	7.813E-004	2	3.907E-004	6.69	0.0013
AB	2.874E-003	4	7.186E-004	29.26	< 0.0001	8.730E-003	4	2.183E-003	37.35	< 0.0001
AC	1.179E-005	4	2.948E-006	0.12	**0.9753**	5.434E-005	4	1.359E-005	0.23	**0.9201**
AD	0.047	4	0.012	473.52	< 0.0001	0.079	4	0.020	338.27	< 0.0001
AE	0.14	4	0.036	1448.10	< 0.0001	0.28	4	0.070	1193.40	< 0.0001
AF	4.311E-004	4	1.078E-004	4.39	0.0017	4.687E-004	4	1.172E-004	2.01	**0.0921**
BC	2.905E-007	4	7.263E-008	2.958E-003	**1.0000**	2.235E-008	4	5.588E-009	9.564E-005	**1.0000**
BD	2.422E-003	4	6.055E-004	24.66	< 0.0001	2.465E-003	4	6.162E-004	10.55	< 0.0001
BE	6.956E-003	4	1.739E-003	70.81	< 0.0001	8.669E-003	4	2.167E-003	37.09	< 0.0001
BF	8.325E-006	4	2.081E-006	0.085	**0.9871**	2.355E-006	4	5.888E-007	0.010	**0.9998**
CD	1.143E-005	4	2.859E-006	0.12	**0.9767**	1.652E-005	4	4.131E-006	0.071	**0.9909**
CE	3.235E-005	4	8.088E-006	0.33	**0.8583**	5.669E-005	4	1.417E-005	0.24	**0.9142**
CF	3.820E-008	4	9.551E-009	3.889E-004	**1.0000**	1.559E-008	4	3.897E-009	6.670E-005	**1.0000**
DE	1.792E-003	4	4.481E-004	18.25	< 0.0001	6.919E-003	4	1.730E-003	29.60	< 0.0001
DF	9.625E-005	4	2.406E-005	0.98	**0.4178**	1.288E-004	4	3.221E-005	0.55	**0.6982**
EF	3.238E-004	4	8.095E-005	3.30	0.0109	4.540E-004	4	1.135E-004	1.94	**0.1017**
Error	0.016	656	2.456E-005			0.038	656	5.843E-005		
Total SS	0.85	728				1.42	728			

Table 5. ANOVA table for failure probability in OR: A indicates the shape parameter in GEV, B indicates the scale parameter of GEV, C indicates the location parameter of GEV, D means the meanlog of LN, E means the sdlog of LN, and F mean the parameters (i.e. theta) in copula

Parameter	Zhangjiashan					Xianyang				
	SS	DF	MS	F-Value	P-value	SS	DF	MS	F-Value	P-value
A	2.04	2	1.02	39285.40	< 0.0001	3.71	2	1.85	30534.64	< 0.0001
B	0.20	2	0.098	3784.17	< 0.0001	0.26	2	0.13	2165.79	< 0.0001
C	9.466E-004	2	4.733E-004	18.22	< 0.0001	1.811E-003	2	9.054E-004	14.91	< 0.0001
D	0.24	2	0.12	4679.22	< 0.0001	0.30	2	0.15	2498.09	< 0.0001
E	0.60	2	0.30	11626.79	< 0.0001	0.87	2	0.43	7132.20	< 0.0001
F	7.833E-004	2	3.916E-004	15.08	< 0.0001	6.382E-004	2	3.191E-004	5.26	0.0054
AB	0.17	4	0.043	1666.34	< 0.0001	0.27	4	0.069	1128.63	< 0.0001
AC	8.076E-004	4	2.019E-004	7.77	< 0.0001	1.830E-003	4	4.575E-004	7.54	< 0.0001
AD	0.048	4	0.012	465.73	< 0.0001	0.081	4	0.020	335.01	< 0.0001
AE	0.15	4	0.037	1418.17	< 0.0001	0.29	4	0.071	1175.81	< 0.0001
AF	3.442E-004	4	8.604E-005	3.31	0.0106	3.658E-004	4	9.144E-005	1.51	**0.1986**
BC	8.013E-005	4	2.003E-005	0.77	**0.5442**	1.226E-004	4	3.064E-005	0.50	**0.7323**
BD	2.528E-003	4	6.319E-004	24.33	< 0.0001	2.534E-003	4	6.334E-004	10.43	< 0.0001
BE	7.212E-003	4	1.803E-003	69.40	< 0.0001	8.837E-003	4	2.209E-003	36.39	< 0.0001
BF	5.294E-006	4	1.323E-006	0.051	**0.9951**	1.077E-006	4	2.693E-007	4.436E-003	**1.0000**
CD	1.192E-005	4	2.981E-006	0.11	**0.9773**	1.697E-005	4	4.242E-006	0.070	**0.9911**
CE	3.353E-005	4	8.382E-006	0.32	**0.8628**	5.780E-005	4	1.445E-005	0.24	**0.9169**
CF	2.416E-008	4	6.040E-009	2.325E-004	**1.0000**	7.119E-009	4	1.780E-009	2.932E-005	**1.0000**
DE	0.11	4	0.028	1069.79	< 0.0001	0.17	4	0.042	691.60	< 0.0001
DF	7.482E-005	4	1.870E-005	0.72	**0.5784**	9.919E-005	4	2.480E-005	0.41	**0.8026**
EF	2.568E-004	4	6.420E-005	2.47	**0.0435**	3.550E-004	4	8.876E-005	1.46	**0.2121**
Error	0.017	656	2.598E-005			0.040	656	6.071E-005		
Total SS	3.60	728				6.01	728			

Table 6. ANOVA table for failure probability in Kendall: A indicates the shape parameter in GEV, B indicates the scale parameter of GEV, C indicates the location parameter of GEV, D means the meanlog of LN, E means the sdlog of LN, and F mean the parameters (i.e. theta) in copula

Parameter	Zhangjiashan					Xianyang				
	SS	DF	MS	F-Value	P-value	SS	DF	MS	F-Value	P-value
A	0.97	2	0.48	33813.15	< 0.0001	2.08	2	1.04	27047.85	< 0.0001
B	0.096	2	0.048	3349.45	< 0.0001	0.15	2	0.076	1983.83	< 0.0001
C	4.627E-004	2	2.313E-004	16.19	< 0.0001	1.055E-003	2	5.274E-004	13.72	< 0.0001
D	0.11	2	0.057	3987.58	< 0.0001	0.17	2	0.084	2181.53	< 0.0001
E	0.28	2	0.14	9809.61	< 0.0001	0.47	2	0.24	6153.63	< 0.0001
F	0.013	2	6.451E-003	451.42	< 0.0001	0.025	2	0.013	331.58	< 0.0001
AB	0.087	4	0.022	1525.14	< 0.0001	0.16	4	0.041	1066.18	< 0.0001
AC	4.090E-004	4	1.022E-004	7.15	< 0.0001	1.101E-003	4	2.754E-004	7.16	< 0.0001
AD	0.022	4	5.448E-003	381.22	< 0.0001	0.044	4	0.011	286.00	< 0.0001
AE	0.066	4	0.017	1156.06	< 0.0001	0.15	4	0.038	995.79	< 0.0001
AF	2.163E-003	4	5.407E-004	37.84	< 0.0001	5.986E-003	4	1.496E-003	38.93	< 0.0001
BC	4.233E-005	4	1.058E-005	0.74	**0.5645**	7.800E-005	4	1.950E-005	0.51	**0.7304**
BD	1.147E-003	4	2.866E-004	20.06	< 0.0001	1.377E-003	4	3.444E-004	8.96	< 0.0001
BE	3.254E-003	4	8.135E-004	56.93	< 0.0001	4.755E-003	4	1.189E-003	30.93	< 0.0001
BF	2.479E-004	4	6.198E-005	4.34	0.0018	4.939E-004	4	1.235E-004	3.21	0.0126
CD	5.408E-006	4	1.352E-006	0.095	**0.9842**	9.226E-006	4	2.307E-006	0.060	**0.9933**
CE	1.513E-005	4	3.782E-006	0.26	**0.9007**	3.112E-005	4	7.781E-006	0.20	**0.9370**
CF	1.190E-006	4	2.974E-007	0.021	**0.9992**	3.369E-006	4	8.423E-007	0.022	**0.9991**
DE	0.054	4	0.014	950.06	< 0.0001	0.096	4	0.024	623.48	< 0.0001
DF	1.870E-004	4	4.676E-005	3.27	0.0114	3.437E-004	4	8.592E-005	2.24	0.0638
EF	4.113E-004	4	1.028E-004	7.20	< 0.0001	9.130E-004	4	2.282E-004	5.94	0.0001
Error	9.374E-003	656	1.429E-005			0.025	656	3.844E-005		
Total SS	1.72	728				3.40	728			

Table 7. Contributions of parameter uncertainties obtained by three level ANOVA to predictive failure probabilities for a design return period of 200-year and service time of 30-year

Factor	FPand	FPor	FPkendall
A	43.53%	56.67%	56.40%
B	2.12%	5.56%	5.58%
C	0.01%	0.03%	0.03%
D	6.94%	6.67%	6.40%
E	21.18%	16.67%	16.28%
F	0.11%	0.02%	0.76%
Interaction	26.12%	4.72%	5.06%

Figure 1. Framework of the proposed IFC approach.
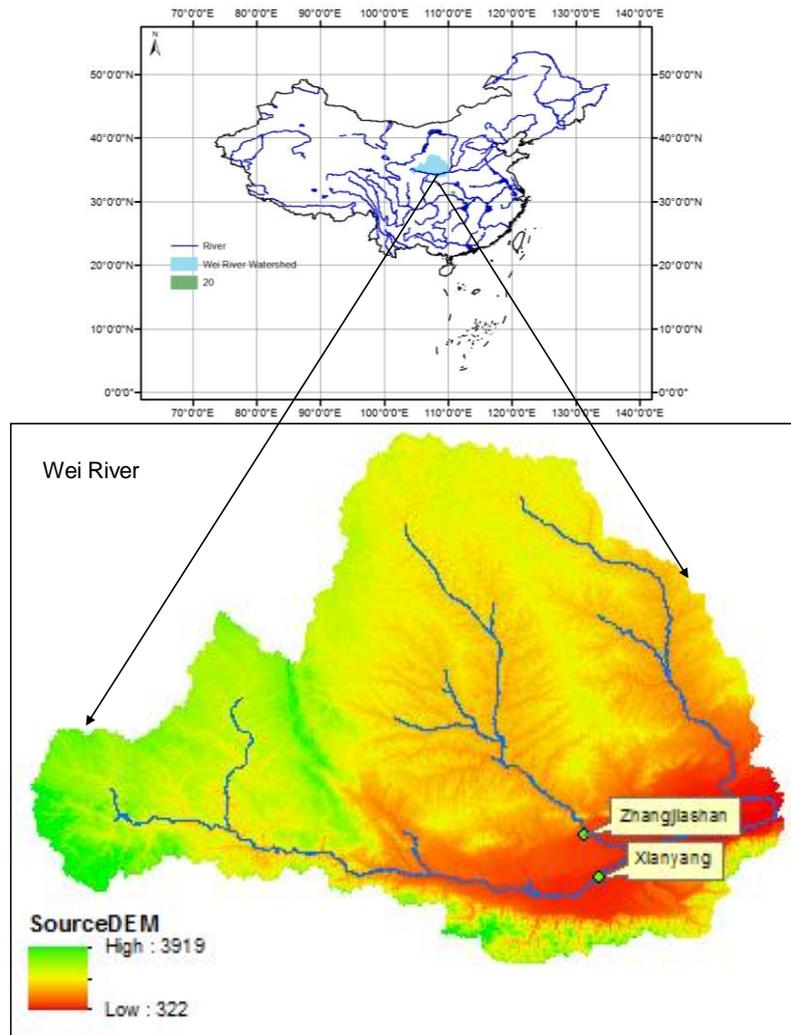
Figure 2. The location of the studied watersheds. Wei River is the largest tributary of Yellow river, with a drainage area of $135,000$ km^2. The historical flood data from Xianyang and Zhangjiashan stations on the Wei River are analyzed through the proposed IFC approach.
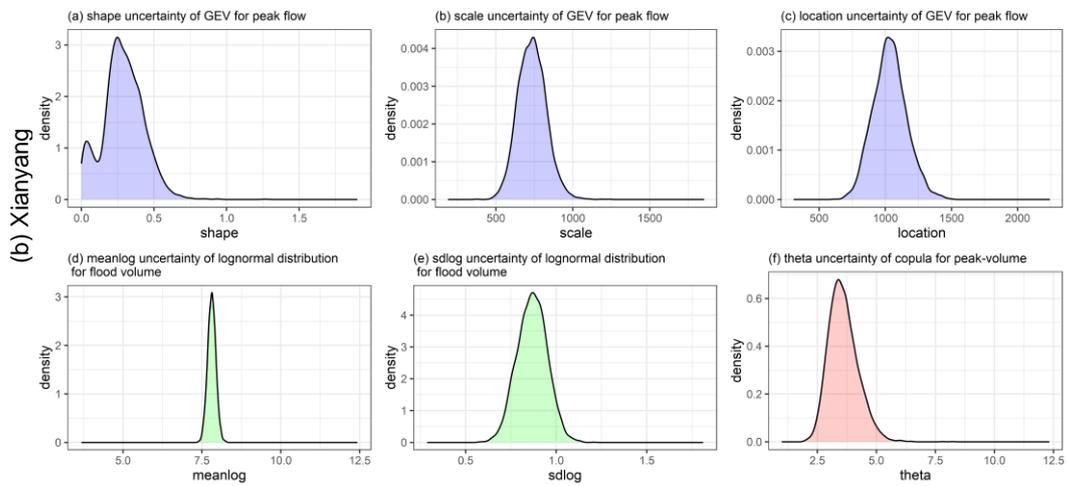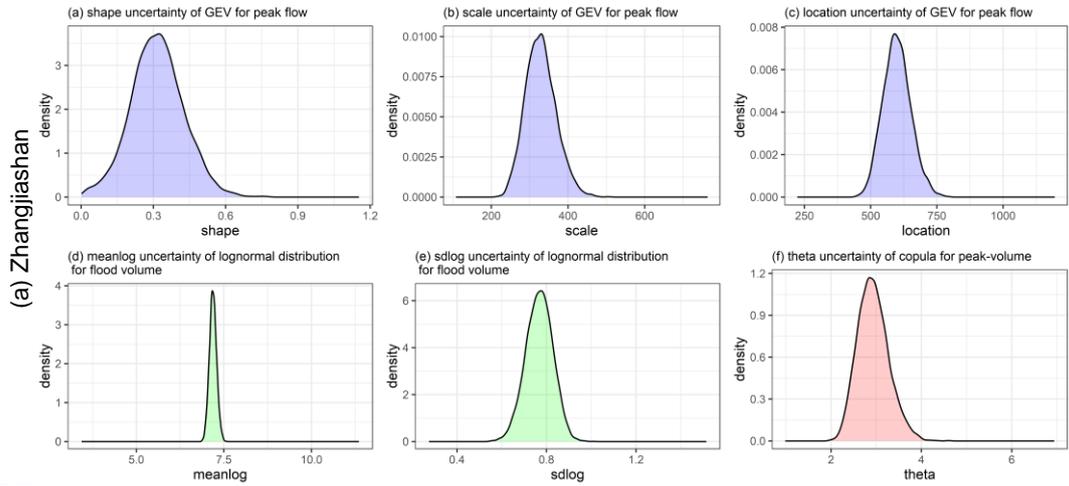
Figure 3. Probabilistic features for parameters in marginal distributions and copula: for both Xianyang and Zhangjiashan stations, the GEV (parameters include shape, scale and location) function would be employed to quantify the distribution of flood peak, while the lognormal distribution (parameters denoted as meanlog and sdlog) is applied for flood volume. The Gumbel and Joe copula (parameter denoted as theta) would be respectively adopted to model the dependence between flood peak and volume at Zhangjiashan and Xianyang stations.

Figure 4. Uncertainty quantification of the joint RP in "AND": the red dash lines indicate the predictive means, the two blue dash lines respectively indicate the 5% and 95% quantiles, and the grey lines indicate the predictions under different parameter samples with the same joint RP of the red and blue dash lines; The cyan lines denote the predictions under different return periods with the model parameters being their mean values.

Figure 5. Uncertainty quantification of the joint RP in "OR": the red dash lines indicate the predictive means, the two blue dash lines respectively indicate the 5% and 95% quantiles, and the grey lines indicate the predictions under different parameter samples with the same joint RP of the red and blue dash lines; The cyan lines denote the predictions under different return periods with the model parameters being their mean values.

Figure 6. Uncertainty quantification of the joint RP in "Kendall": the red dash lines indicate the predictive means, the two blue dash lines respectively indicate the 5% and 95% quantiles, and the grey lines indicate the predictions under different parameter samples with the same joint RP of the red and blue dash lines; The cyan lines denote the predictions under different return periods with the model parameters being their mean values.

Figure 7. Main effects plot and full interactions plot matrix for parameters on the failure probability in AND at the two gauge stations.

Figure 8. Main effects plot and full interactions plot matrix for parameters on the failure probability in OR at the two gauge stations

Figure 9. Main effects plot and full interactions plot matrix for parameters on the failure probability in Kendall at the two gauge stations

		30 year	50 year	70 year	30 year	50 year	70 year
		(a) Zhangjiashan			**(b) Xianyang**		
RP: 200	GEV_shape	45.83%	46.37%	46.88%	49.26%	50.15%	50.99%
	GEV_scale	4.93%	4.96%	5.00%	2.27%	2.24%	2.21%
	GEV_location	0.05%	0.05%	0.05%	0.03%	0.03%	0.03%
	LN_meanlog	10.22%	10.21%	10.19%	8.30%	8.24%	8.19%
	LN_sdlog	23.61%	23.67%	23.70%	23.02%	23.08%	23.11%
	Cop_theta	0.23%	0.23%	0.22%	0.11%	0.10%	0.10%
	Par_interaction	15.14%	14.52%	13.96%	17.02%	16.16%	15.38%
RP: 300	GEV_shape	45.86%	46.30%	46.73%	47.74%	48.40%	49.04%
	GEV_scale	4.04%	4.05%	4.06%	1.95%	1.93%	1.91%
	GEV_location	0.03%	0.03%	0.03%	0.02%	0.02%	0.02%
	LN_meanlog	9.44%	9.43%	9.41%	7.83%	7.78%	7.73%
	LN_sdlog	23.96%	24.03%	24.08%	23.70%	23.79%	23.86%
	Cop_theta	0.18%	0.18%	0.17%	0.09%	0.08%	0.08%
	Par_interaction	16.48%	15.98%	15.51%	18.68%	18.00%	17.36%
RP: 500	GEV_shape	45.50%	45.82%	46.13%	45.77%	46.22%	46.65%
	GEV_scale	3.22%	3.22%	3.21%	1.71%	1.69%	1.67%
	GEV_location	0.02%	0.02%	0.02%	0.01%	0.01%	0.01%
	LN_meanlog	8.66%	8.65%	8.63%	7.36%	7.32%	7.28%
	LN_sdlog	24.38%	24.44%	24.50%	24.43%	24.52%	24.61%
	Cop_theta	0.14%	0.14%	0.13%	0.07%	0.07%	0.06%
	Par_interaction	18.09%	17.72%	17.37%	20.65%	20.18%	19.71%

Legend: 1% | 10% | 20% | 30% | 40% | 50%

Figure 10. Contributions of parameter uncertainties to predictive failure probabilities in AND under different design standards (i.e. return periods (RP)) and different service periods

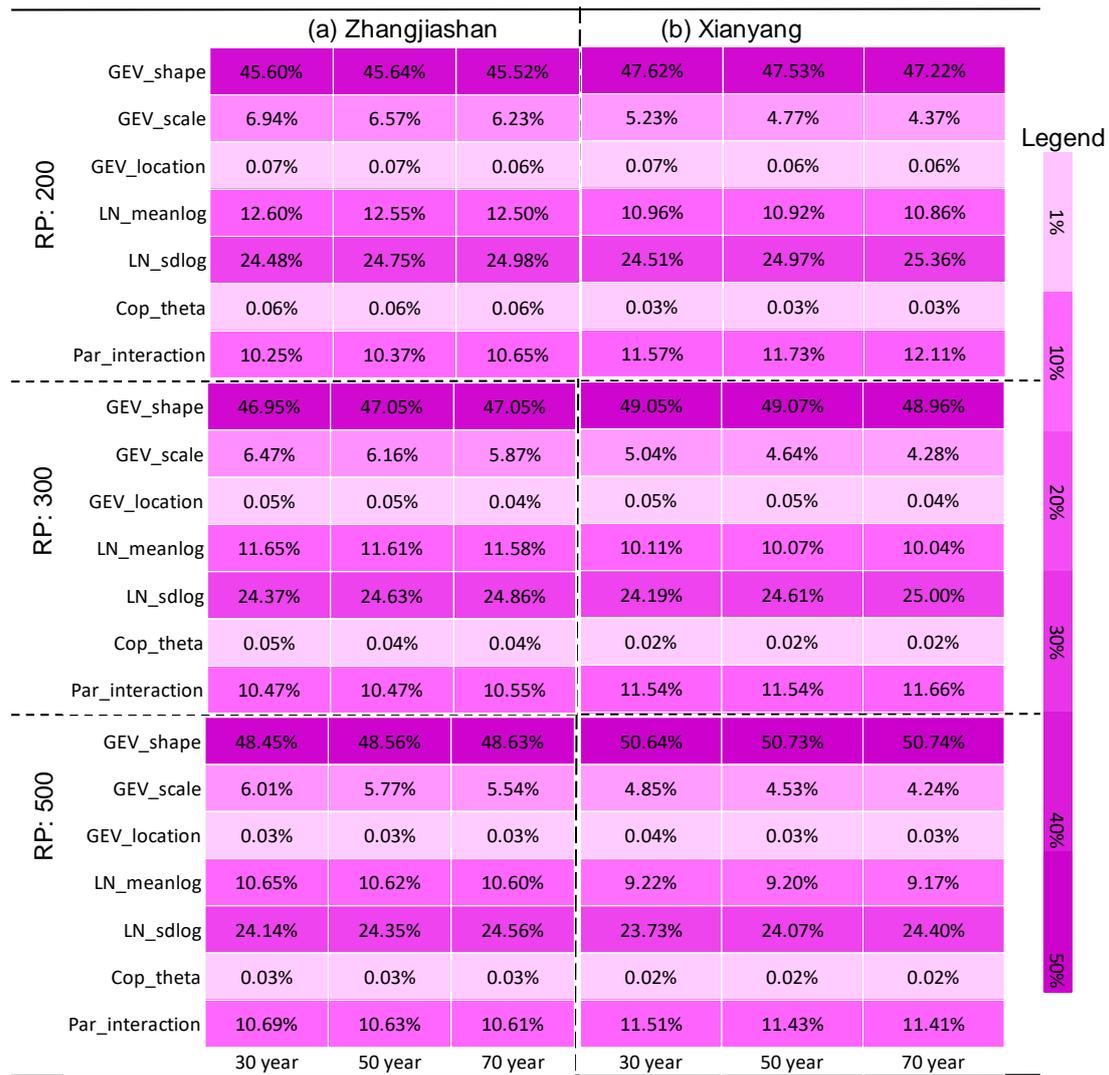|		(a) Zhangjiashan			(b) Xianyang		
		30 year	50 year	70 year	30 year	50 year	70 year
RP: 200	GEV_shape	45.60%	45.64%	45.52%	47.62%	47.53%	47.22%
	GEV_scale	6.94%	6.57%	6.23%	5.23%	4.77%	4.37%
	GEV_location	0.07%	0.07%	0.06%	0.07%	0.06%	0.06%
	LN_meanlog	12.60%	12.55%	12.50%	10.96%	10.92%	10.86%
	LN_sdlog	24.48%	24.75%	24.98%	24.51%	24.97%	25.36%
	Cop_theta	0.06%	0.06%	0.06%	0.03%	0.03%	0.03%
	Par_interaction	10.25%	10.37%	10.65%	11.57%	11.73%	12.11%
RP: 300	GEV_shape	46.95%	47.05%	47.05%	49.05%	49.07%	48.96%
	GEV_scale	6.47%	6.16%	5.87%	5.04%	4.64%	4.28%
	GEV_location	0.05%	0.05%	0.04%	0.05%	0.05%	0.04%
	LN_meanlog	11.65%	11.61%	11.58%	10.11%	10.07%	10.04%
	LN_sdlog	24.37%	24.63%	24.86%	24.19%	24.61%	25.00%
	Cop_theta	0.05%	0.04%	0.04%	0.02%	0.02%	0.02%
	Par_interaction	10.47%	10.47%	10.55%	11.54%	11.54%	11.66%
RP: 500	GEV_shape	48.45%	48.56%	48.63%	50.64%	50.73%	50.74%
	GEV_scale	6.01%	5.77%	5.54%	4.85%	4.53%	4.24%
	GEV_location	0.03%	0.03%	0.03%	0.04%	0.03%	0.03%
	LN_meanlog	10.65%	10.62%	10.60%	9.22%	9.20%	9.17%
	LN_sdlog	24.14%	24.35%	24.56%	23.73%	24.07%	24.40%
	Cop_theta	0.03%	0.03%	0.03%	0.02%	0.02%	0.02%
	Par_interaction	10.69%	10.63%	10.61%	11.51%	11.43%	11.41%

Legend

1%
10%
20%
30%
40%
50%

Figure 11. Contributions of parameter uncertainties to predictive failure probabilities in OR under different design standards (i.e. return periods (RP)) and different service periods

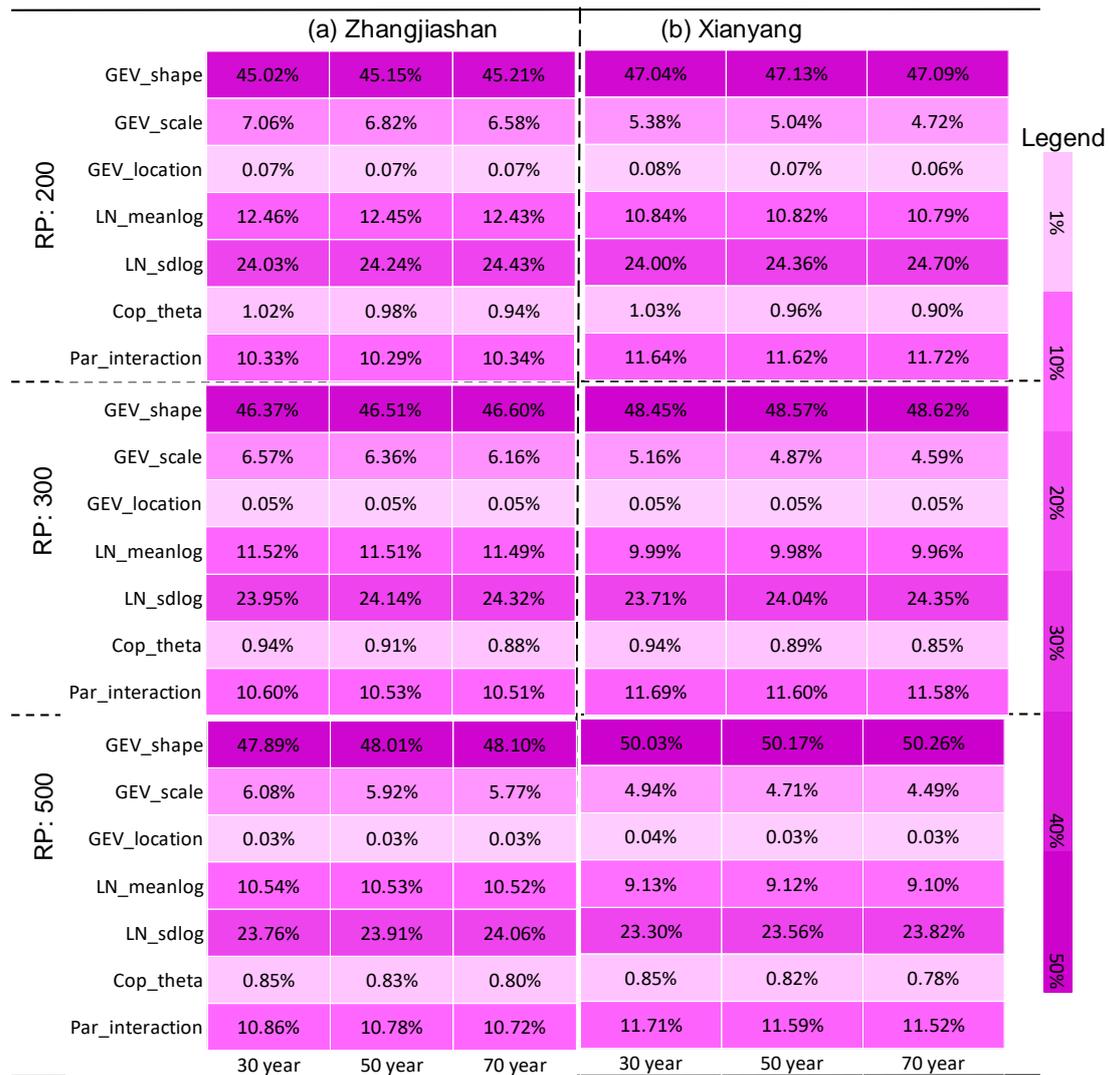|	(a) Zhangjiashan			(b) Xianyang		
RP: 200						
GEV_shape	45.02%	45.15%	45.21%	47.04%	47.13%	47.09%
GEV_scale	7.06%	6.82%	6.58%	5.38%	5.04%	4.72%
GEV_location	0.07%	0.07%	0.07%	0.08%	0.07%	0.06%
LN_meanlog	12.46%	12.45%	12.43%	10.84%	10.82%	10.79%
LN_sdlog	24.03%	24.24%	24.43%	24.00%	24.36%	24.70%
Cop_theta	1.02%	0.98%	0.94%	1.03%	0.96%	0.90%
Par_interaction	10.33%	10.29%	10.34%	11.64%	11.62%	11.72%
RP: 300						
GEV_shape	46.37%	46.51%	46.60%	48.45%	48.57%	48.62%
GEV_scale	6.57%	6.36%	6.16%	5.16%	4.87%	4.59%
GEV_location	0.05%	0.05%	0.05%	0.05%	0.05%	0.05%
LN_meanlog	11.52%	11.51%	11.49%	9.99%	9.98%	9.96%
LN_sdlog	23.95%	24.14%	24.32%	23.71%	24.04%	24.35%
Cop_theta	0.94%	0.91%	0.88%	0.94%	0.89%	0.85%
Par_interaction	10.60%	10.53%	10.51%	11.69%	11.60%	11.58%
RP: 500						
GEV_shape	47.89%	48.01%	48.10%	50.03%	50.17%	50.26%
GEV_scale	6.08%	5.92%	5.77%	4.94%	4.71%	4.49%
GEV_location	0.03%	0.03%	0.03%	0.04%	0.03%	0.03%
LN_meanlog	10.54%	10.53%	10.52%	9.13%	9.12%	9.10%
LN_sdlog	23.76%	23.91%	24.06%	23.30%	23.56%	23.82%
Cop_theta	0.85%	0.83%	0.80%	0.85%	0.82%	0.78%
Par_interaction	10.86%	10.78%	10.72%	11.71%	11.59%	11.52%
	30 year	50 year	70 year	30 year	50 year	70 year

Legend: 1% 10% 20% 30% 40% 50%

Figure 12. Contributions of parameter uncertainties to predictive failure probabilities in Kendall under different design standards (i.e. return periods (RP)) and different service periods

		(a) 3-Level			(b) 4-Level		
FPand	GEV_shape	45.83%	46.37%	46.88%	51.52%	51.93%	52.32%
	GEV_scale	4.93%	4.96%	5.00%	6.09%	6.11%	6.13%
	GEV_location	0.05%	0.05%	0.05%	0.06%	0.06%	0.06%
	LN_meanlog	10.22%	10.21%	10.19%	7.95%	7.92%	7.89%
	LN_sdlog	23.61%	23.67%	23.70%	19.96%	19.92%	19.86%
	Cop_theta	0.23%	0.23%	0.22%	0.27%	0.27%	0.27%
	Par_interaction	15.14%	14.52%	13.96%	14.14%	13.80%	13.47%
FPor	GEV_shape	45.60%	45.64%	45.52%	39.28%	39.35%	39.38%
	GEV_scale	6.94%	6.57%	6.23%	6.86%	6.70%	6.54%
	GEV_location	0.07%	0.07%	0.06%	0.07%	0.07%	0.07%
	LN_meanlog	12.60%	12.55%	12.50%	14.25%	14.19%	14.13%
	LN_sdlog	24.48%	24.75%	24.98%	29.82%	29.95%	30.05%
	Cop_theta	0.06%	0.06%	0.06%	0.08%	0.08%	0.08%
	Par_interaction	10.25%	10.37%	10.65%	9.62%	9.66%	9.75%
FPkendall	GEV_shape	45.02%	45.15%	45.21%	38.87%	38.94%	39.00%
	GEV_scale	7.06%	6.82%	6.58%	6.89%	6.78%	6.68%
	GEV_location	0.07%	0.07%	0.07%	0.07%	0.07%	0.07%
	LN_meanlog	12.46%	12.45%	12.43%	14.13%	14.10%	14.06%
	LN_sdlog	24.03%	24.24%	24.43%	29.45%	29.55%	29.64%
	Cop_theta	1.02%	0.98%	0.94%	0.92%	0.90%	0.88%
	Par_interaction	10.33%	10.29%	10.34%	9.68%	9.66%	9.66%
		30 year	50 year	70 year	30 year	50 year	70 year

Legend

1%
10%
20%
30%
40%
50%

Figure 13. Comparison of parameter contributions to predictive uncertainty for failure probabilities under different levels of subsampling for Zhangjiashan station: three (i.e. 0.1, 0.5, 0.9) and four (i.e. 0.1, 0.35, 0.6, 0.85) level quantiles are adopted for subsampling and the design return period is 200 years.
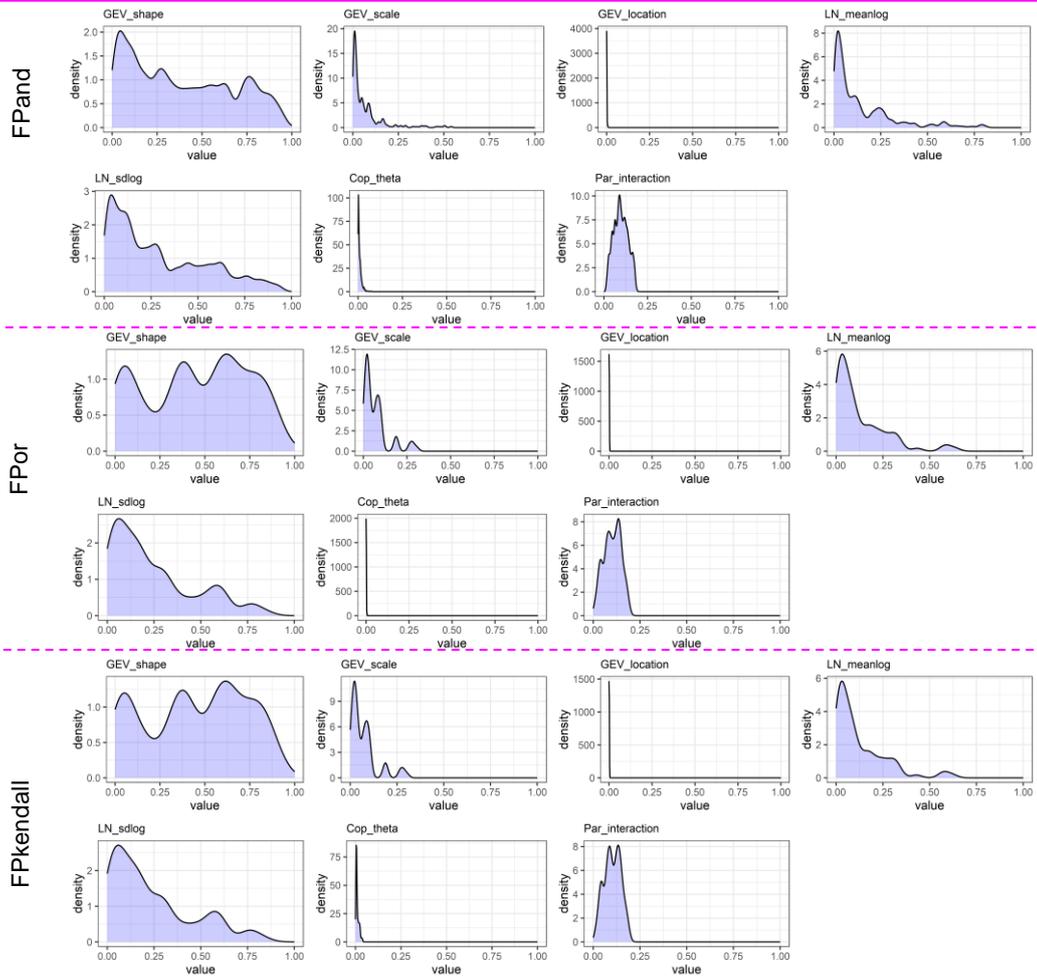
Figure 14. Variation of parameters' contributions for different risk inferences at the Zhangjiashan Station for a design standard of 200-year and a service time of 30-year

Figure 15. Correlation for parameters' contributions on risk inferences at Zhangjiashan station for a design standard of 200-year and a service time of 30-year: The cross sign indicates the correlation is statistically insignificant.